

DESIGN AND DEVELOPMENT OF A HIGH-POWER ROCKET USING COMPOSITE MATERIALS

ME3811 - PROJECT WORK

Submitted by

VENKATESHA RISHI A	910021114048
VENKATESH A M	910021114049
SANJAY ROOPAN S	910021114036
NISANTHALAL M J	910021114029

in partial fulfillment for the award of the degree of

BACHELOR OF ENGINEERING

in

MECHANICAL ENGINEERING



ANNA UNIVERSITY, REGIONAL CAMPUS

MADURAI - 625019

ANNA UNIVERSITY: CHENNAI 600 025

MAY 2025

ANNA UNIVERSITY: CHENNAI - 600025

BONAFIDE CERTIFICATE

Certified that this project report titled **”DESIGN AND DEVELOPMENT OF A HIGH-POWER ROCKET USING COMPOSITE MATERIALS”** is the bonafide work of VENKATESHA RISHI A - 910021114048, VENKATESH A M - 910021114049, SANJAY ROOPAN S - 910021114036, NISANTHALAL M J - 910021114029 who carried out the project under my supervision.

SIGNATURE

HEAD OF THE DEPARTMENT

Dr.S.Sudhakar

Assistant Professor

Department of Mechanical Engineering

Anna University Regional Campus

Madurai - 625019

SIGNATURE

PROJECT SUPERVISOR

Mr.B.J Ashok Kumar

Teaching Fellow

Department of Mechanical Engineering

Anna University Regional Campus

Madurai - 625019

Submitted for the project viva-voice examination held on _____

Internal Examiner

External Examiner

ABSTRACT

In a time where space exploration is often confined to billion-dollar agencies and high-end facilities, this project represents a bold step towards democratizing rocketry through ingenuity, sustainability, and resourcefulness. This study documents the complete design, fabrication, and testing of a high-power rocket built using kraft paper-based composite materials and a homemade solid propellant composed of potassium nitrate and glucose. Developed entirely by a small student team with minimal resources, the rocket was engineered to achieve substantial thrust and structural performance while remaining environmentally conscious and cost-effective.

Core systems including a custom-made de Laval nozzle, modular payload bay, and a parachute-based recovery mechanism were integrated using lightweight, low-cost materials without compromising on reliability. The propulsion system underwent rigorous static ground testing to validate burn stability, pressure response, and overall mechanical integrity. Furthermore, a simple yet effective electronics suite was employed to facilitate future implementation of sensing, tracking, and telemetry solutions.

The challenges posed by legal, ethical, and logistical constraints—especially within the Indian aerospace context were met with caution, innovation, and an unwavering commitment to safe practices. In doing so, this project not only serves as a proof of concept for affordable, student-led rocket engineering, but also as a powerful inspiration: that space-bound dreams need not wait for billion-dollar budgets they can ignite from paper, patience, and purpose.

ACKNOWLEDGEMENT

We take this opportunity to express our deepest gratitude to all those who contributed to the successful completion of this project, both directly and indirectly.

First and foremost, we extend our sincere thanks to our teaching staff and project advisor, **Mr.B.J Ashok Kumar**, from the Department of Mechanical Engineering, Anna University Regional Campus, Madurai, for his invaluable guidance, continuous support, and constructive feedback throughout every phase of the project. His mentorship was instrumental in helping us transform our initial ideas into a functioning high-power rocket system.

We are equally grateful to our respected Head of the Department, **Dr.S.Sudhakar**, Department of Mechanical Engineering, for fostering a supportive academic environment and encouraging us to take up such a challenging and ambitious project.

We would also like to express our heartfelt thanks to all the teaching and non-teaching staff of the Mechanical Engineering Department for their assistance and encouragement. Their technical inputs and logistical support were crucial during the various stages of fabrication and testing.

Special thanks are also due to the faculty and lab technicians from other departments, who offered us access to their tools, knowledge, and time whenever we sought interdisciplinary help. Their willingness to collaborate played a vital role in overcoming practical hurdles in electronics integration, testing instrumentation, and material processing.

We would also like to thank our classmates and friends for standing by us through the demanding phases of design, simulation, prototyping, and static testing. Their moral support, collaboration, and occasional hands-on help kept us motivated and focused. Finally, we extend our deepest appreciation to our families for their constant support, patience, and encouragement, without which this journey would not have been possible.

This project was not just an academic venture it was a culmination of teamwork, learning, and perseverance. We are truly grateful to everyone who contributed to this achievement.

VENKATESHA RISHI A	VENKATESH A M	SANJAY ROOPAN S	NISANTHALAL M J
910021114048	910021114049	910021114036	910021114029

TABLE OF CONTENTS

ABSTRACT	ii
ACKNOWLEDGEMENT	iii
TABLE OF CONTENTS	iv
LIST OF FIGURES	vi
ABBREVIATIONS	vii
1 Introduction	1
1.1 Problem Definition	2
2 Literature Review	4
2.1 Model Rocketry with Sugar-Based Propellants	4
2.2 Kraft-Based and Phenolic Composite Structures in Rocketry	5
2.3 Recovery Systems in High-Power Amateur Rockets	5
2.4 Simulation Tools and Performance Prediction	7
3 Objectives	9
3.1 Development of a High-Altitude Rocket Using Kraft Phenolic Composite	9
3.2 Development of a Single-Use, Modular KNO_3 –Glucose Solid Propellant Grain System	9
3.3 Integration of an Ejection-Based Recovery and Payload Deployment System	10
3.4 Validate Performance Through Simulation and Ground Testing	11
4 Functional Requirements	12
5 Design Approach	14
5.1 Aerodynamics and Structures	15
5.1.1 Nose Cone	16
5.1.2 Fins	18
5.1.3 Couplers	19
5.1.4 Body	20
5.1.5 Nozzle Design	25
6 Mechatronics and Controls	28
6.1 Electronics	28
6.2 Aviation Bay	28
6.3 Parachute Deployment	29

6.4	Theoretical and Practical Analysis	30
6.5	Parachute Material and Design	31
6.6	System Integration and Safety Considerations	31
7	Propulsion	32
8	Methodology	36
8.1	Prototype	38
8.1.1	Manufacturing and Fabrication	39
8.1.2	Propulsion Preparation	45
8.1.3	Parachute Deployment System	47
8.1.4	Electronics and Telemetry Systems	48
8.1.5	Integration	49
9	Testing Results	52
9.1	Introduction	52
9.2	Static Testing Setup	53
9.3	Instrumentation and Measurement Systems	54
9.4	Test Procedures	55
9.4.1	Static Testing Protocol	55
9.4.2	Safety Protocols Implemented	56
9.4.3	Parameters Monitored During Test	56
9.5	Results and Analysis	57
9.5.1	Static Test Results	57
9.5.2	Analytical Evaluation	59
9.5.3	Discussion	60
10	Challenges	61
10.1	Risk and Liability	61
10.2	Ethical Issues	62
10.3	Impact on Society	63
10.4	Impact on the Environment	64
11	Conclusion	66
	References	67

List of Figures

5.1	Nose Cone Concet model from Blender	16
5.2	Nose Cone Data from Open Rocket	17
5.3	Comparison of Four Nose Cone Shapes	17
5.4	Nose cone comparison	17
5.5	Fin Concept model from Blender	18
5.6	Different Fin Designs	19
5.7	Fin Set data from Open Rocket	19
5.8	Coupler data from Open Rocket	20
5.9	First Body data from Open Rocket	21
5.10	Second Body data from Open Rocket	21
5.11	Body Concept model from blender	22
5.12	Body with fins concept model from blender	23
5.13	Rocket data from open rocket	24
5.14	Full rocket Concept model from blender	24
5.15	Nozzle data	25
5.16	Motor Characteristic	27
5.17	Motor Characteristic from open motor	27
7.1	KN calculation	33
7.2	KN vs Web regression	34
8.1	Conept Model from blender	37
8.2	Rocket Art from Blender	38
8.3	Rocket Concept art from open rocket	39
8.4	Nose	40
8.5	Body of the Prototype	41
8.6	Fins	43
8.7	Motor along with the nozzle	44
8.8	Parachute	48
8.9	Rocket Assembly	51
9.1	Roll characteristics	58
9.2	Stability vs Time	58
9.3	Vertical motion vs Time	59
10.1	Concept Art 1	64
10.2	Concept Art 2	65

ABBREVIATION

KNO3	Potassium Nitrate
KNSU	Potassium Nitrate Sucrose
KNSB	Potassium Nitrate Sorbitol
BATES	Ballistic Test and Evaluation System
NASA	National Aeronautics and Space Administration
ISRO	Indian Space Research Organisation
GPS	Global Positioning System
CG	Center of Gravity
CP	Center of Pressure
SRAD	Student Researched and Developed
IMU	Inertial Measurement Unit
SD	Secure Digital
3FG	Three-Fin Geometry
4FG	Four-Fin Geometry
CO	Carbon Monoxide
PCB	Printed Circuit Board
CAD	Computer-Aided Design
ESP32	Espressif Systems Microcontroller
Wi-Fi	Wireless Fidelity
MPU	Motion Processing Unit
BMP	Barometric Pressure Sensor
DAQ	Data Acquisition
ESD	Electrostatic Discharge

FFT Fast Fourier Transform

MTCR Missile Technology Control Regime

DGCA Directorate General of Civil Aviation

DRDO Defence Research and Development Organisation

STEM Science, Technology, Engineering, and Mathematics

CHAPTER 1: Introduction

This project revolves around the design and development of a high-power, single-stage model rocket capable of reaching impressive altitudes approaching 1500 meters, powered entirely by a hand-crafted solid fuel system. The rocket was conceived and constructed from the ground up using an unconventional approach that favored affordability, accessibility, and innovation over industrial-grade materials or commercial components. Central to this project is the use of a kraft phenolic composite material—an inexpensive, lightweight, and surprisingly durable alternative to carbon fiber. This composite offers a significant advantage: while it lacks the extreme tensile strength of carbon fiber, it is easier to work with, more cost-effective for student-led development, and capable of withstanding the thermal and mechanical loads encountered during high-speed flight.

The body of the rocket, including its fins, rings, and structural segments, was hand-fabricated using this kraft phenolic composite, which allowed for fine customization of part geometry and internal fittings. This also made it possible to achieve tight tolerances essential for stability and recovery system integration. The rocket's design places emphasis on aerodynamic efficiency and structural resilience, featuring a long ogive-shaped nose cone that minimizes drag while maintaining internal volume for avionics and payload.

Unlike conventional model rockets that rely on commercial motors, this project uses a self-formulated solid propellant made from potassium nitrate and glucose. This sugar-based fuel, sometimes referred to as "rocket candy," was selected for its relatively simple preparation process, high energy output, and ease of shaping into modular fuel grains. One of the most unique aspects of this design is the inclusion of a replaceable fuel canister system, which allows for rapid reloading and experimentation with different grain geometries and burn profiles. This modularity in the propulsion system makes it ideal for educational purposes, enabling repeated ground testing and gradual performance optimization.

The propulsion system was carefully designed to be compatible with the recovery mechanism. The internal pressure build-up from combustion is utilized to trigger the ejection of a dual-stage recovery system, consisting of a shock-cord-linked payload bay, a drogue chute, and a main parachute. This integration ensures that the recovery sequence is synchronized with apogee, thereby reducing landing speed and minimizing structural damage. Every aspect of the rocket—from the fin geometry and coupler placement to the mass distribution and thrust-to-weight ratio—was simulated using OpenRocket. These simulations helped validate design decisions and refine stability margins, taking into account the unique burn characteristics of the hand-made propellant.

Through this project, we explored an approach that relies less on expensive aerospace-grade materials and more on fundamental principles of aerodynamics, chemistry, and mechanical design. The result is a high-power rocket system that is robust, modular, and built almost entirely with hand-

crafted components. In an academic environment where access to advanced manufacturing equipment is limited, this project demonstrates that intelligent material selection, careful design, and iterative testing can produce a vehicle that rivals more expensive alternatives in performance, while remaining entirely student-built and ground tested.

1.1 Problem Definition

The central problem addressed by this project is how to design, fabricate, and successfully launch a high-power model rocket using non-conventional, low-cost materials without compromising structural integrity, flight performance, or safety. Traditional model rockets often rely on precision-manufactured components and aerospace-grade materials such as fiberglass, carbon composites, or aluminum alloys. These are expensive, require specialized equipment to work with, and are often inaccessible in a university setting without significant financial backing. In contrast, our team has chosen to develop the rocket using a kraft-paper-like laminated fiber-cellulose composite—a material more commonly associated with packaging—aiming to push the boundaries of what such materials can achieve in aerospace applications.

The problem extends far beyond just selecting a cheap material. A rocket undergoes extreme mechanical and thermal stress during its operation. From the moment of ignition, the propulsion system produces rapid accelerations, heat, and vibration. These factors place tremendous strain on the rocket's body, joints, and components. The material used must not only withstand these forces but also maintain dimensional stability so that the rocket remains aerodynamically stable throughout the flight. Using a fiber-based composite introduces risks such as delamination, moisture absorption, and buckling under pressure—all of which had to be accounted for through intelligent design choices, reinforcement strategies, and rigorous testing.

Furthermore, the rocket is required to carry a payload—potentially for atmospheric sensing or data collection—requiring the design to accommodate a modular payload bay. This adds additional weight and complexity, especially in a structure that is already pushing the limits of its material strength. Simultaneously, the rocket must also incorporate a reliable recovery mechanism. Without it, the risk of crash-landing increases, which could damage the rocket beyond reuse or pose a safety hazard. The inclusion of a parachute-based deployment system adds yet another layer of engineering complexity, particularly when dealing with passive triggers or small ejection charges that must activate at a specific point in the flight.

Designing the rocket is not a matter of assembling separate parts in isolation; each component directly affects others. For example, the dimensions and shape of the nose cone influence drag and therefore affect the size and placement of fins needed for stability. These, in turn, shift the rocket's center of pressure, which must always remain behind the center of gravity to ensure stable flight. These relationships forced us to adopt an iterative design process, where changes in one part necessitated recalculations and often physical redesigns of other components. The material's behavior, especially

under load, introduced further complications, as real-world performance sometimes deviated from analytical predictions. Adding to these challenges was the decision to fabricate all major components in-house. Unlike some academic programs that outsource parts to professional suppliers, we intentionally chose a hands-on approach to deepen our understanding of each step in the development process. This decision meant building the nose cone, fins, motor casing, and avionics bay ourselves, using only basic tools and workshop equipment. As a result, the team faced steep learning curves in terms of precision fabrication, curing of composites, and maintaining symmetry in rotating parts.

In essence, this project takes on a multi-faceted engineering challenge: to deliver a functioning, high-power rocket made from an unorthodox material, designed and constructed entirely by undergraduate students, and capable of performing a real-world test flight with recoverability and payload compatibility. The problem, therefore, is not just technical—it is logistical, educational, and experimental in nature. It tests our ability to translate theoretical knowledge into a functioning aerospace system under material, financial, and time constraints.

CHAPTER 2: Literature Review

2.1 Model Rocketry with Sugar-Based Propellants

Sugar-based solid propellants, often referred to as “candy propellants,” are widely used in the experimental and amateur rocketry community due to their affordability, availability, and relatively safe handling characteristics. The most common formulation involves a mixture of potassium nitrate (KNO_3) as the oxidizer and a sugar (such as sucrose, dextrose, or glucose) as the fuel. This combination is known as KNSU (potassium nitrate–sucrose) or more generally KNSB when variations like glucose are used. The glucose-based version was chosen for our project due to its lower melting point and easier handling during the casting process.

The works of Richard Nakka, a pioneer in sugar-propellant research, laid the foundation for understanding how different ratios, casting techniques, and grain geometries affect burn performance and internal chamber pressures. His tests showed that sugar propellants, when properly processed, can generate enough thrust to reach several kilometers in altitude, rivaling low-end commercial motors. This performance, coupled with low toxicity and the absence of specialized manufacturing requirements, makes sugar propellants especially attractive for academic and hobbyist rocket projects.

Further experimentation by online research communities and academic groups (such as those documented on forums like The Rocketry Forum and in publications from amateur engineering projects) has refined grain designs like BATES, core-burn, and end-burn configurations. These studies emphasize burn rate control, structural containment, and nozzle efficiency—all critical to prevent overpressurization and ensure consistent thrust.

Our own propulsion system draws directly from this body of research. We selected a glucose- KNO_3 mixture, hand-cast into a phenolic composite casing. The cylindrical grain design and nozzle were optimized through OpenMotor simulation, ensuring compatibility with the body tube and predicted apogee. Unlike commercial motors, this hand-crafted propellant system is tailored to match our custom-made ejection system and recovery compartment, allowing for full mission flexibility without dependency on commercially rated thrust or delay timings.

This body of literature firmly supports the practicality of using sugar propellants for high-performance, low-cost rocketry, especially when paired with simulation tools and modular design practices like ours.

2.2 Kraft-Based and Phenolic Composite Structures in Rocketry

The use of kraft-based and phenolic composites in rocket structural components represents an innovative approach, particularly in the context of cost-effectiveness and manufacturing simplicity. Unlike traditional materials such as carbon fiber composites, fiberglass, or metals like aluminum and titanium, kraft phenolic composites offer a unique balance of mechanical strength, thermal resistance, and affordability.

Phenolic resins are well-known for their excellent heat resistance and low flammability, properties essential for components exposed to high thermal loads during rocket launches. When combined with kraft paper, a natural cellulose fiber, these composites provide sufficient structural integrity for medium to high-power rocketry applications without the high cost and complex fabrication techniques demanded by carbon fiber or metal alloys.

One key advantage of kraft phenolic composites is their environmental friendliness and ease of handling. Kraft paper is a renewable resource, and its integration into phenolic resin matrices reduces reliance on petroleum-based synthetic fibers. This translates into a more sustainable manufacturing process with lower embodied energy compared to carbon fiber production, which is energy-intensive and expensive.

NASA's research into phenolic composites has historically validated their use in heat shields, ablative coatings, and structural parts of spacecraft and sounding rockets. The material's ability to maintain strength at elevated temperatures, resist chemical degradation, and provide good mechanical stiffness has made phenolic composites a go-to choice in certain aerospace applications. While NASA predominantly uses high-performance carbon composites for critical load-bearing parts, phenolic-based composites are often employed for thermal protection systems and components where cost and thermal stability are prioritized over ultra-high strength.

In our project, using kraft phenolic composites for the rocket's body tubes, nose cone, and fins was a strategic decision driven by these proven advantages. Compared to carbon fiber, our chosen material provides sufficient strength and stiffness for the intended flight envelope, better thermal tolerance during motor ignition, and significantly reduced costs. Moreover, the ease of fabrication through epoxy impregnation and curing enables rapid prototyping and repair, essential for a student-led experimental program.

Thus, this composite structure aligns well with the goals of producing a reliable, cost-effective, and sustainable rocket, with credible precedents in aerospace research and practical field use.

2.3 Recovery Systems in High-Power Amateur Rockets

Recovery systems play a crucial role in the design and operation of high-power amateur rockets, serving as the primary means to ensure the safe return of the rocket and its valuable components

after flight. Unlike smaller model rockets, high-power rockets reach greater altitudes and velocities, which significantly increases the risk of damage upon landing if proper recovery methods are not employed. Consequently, the development and optimization of effective recovery systems have been a focal point of amateur rocketry research and practice.

The most common recovery mechanism involves the deployment of parachutes, which slow the rocket's descent by increasing drag and reducing terminal velocity to a non-destructive level. Typically, multi-stage recovery systems are used to manage different phases of descent. For instance, a drogue parachute may be deployed immediately after the rocket reaches apogee to stabilize and slow it during the initial, faster descent phase. Following this, a larger main parachute is deployed at a lower altitude to further reduce descent speed, ensuring a gentle touchdown.

The design and timing of these deployments are critical. Deployment must occur at precise moments to avoid damage to the rocket structure or payload and to prevent premature opening that could destabilize the rocket during ascent. Advanced electronics such as altimeters, barometric sensors, or accelerometers are often integrated to detect apogee and trigger ejection charges that deploy parachutes. These electronics are carefully selected and tested to withstand the dynamic flight environment, including acceleration, vibration, and thermal conditions.

The materials chosen for parachutes and recovery components also impact the effectiveness and reliability of the recovery system. Ripstop nylon is widely favored due to its high strength-to-weight ratio, durability, and resistance to tearing. The use of braided nylon or Kevlar cords for shroud lines ensures secure attachment between the parachute canopy and rocket body, with minimal risk of line failure during deployment stresses.

In recent years, amateur rocketry enthusiasts and organizations such as the National Association of Rocketry (NAR) and Tripoli Rocketry Association have published extensive guidelines and best practices to improve recovery system designs. These include recommendations for parachute sizing based on rocket mass and descent velocity, shock cord specifications, and ejection charge calculations. The development of reliable recovery systems not only protects physical assets but also promotes safety in rocketry activities, reducing hazards to people and property near launch sites.

Furthermore, innovations have emerged in recovery technologies, such as the use of dual-deployment systems where both drogue and main parachutes are employed, GPS tracking devices for easier rocket retrieval, and telemetry systems that transmit live flight data including altitude and velocity. These advancements reflect an ongoing effort to enhance the efficiency, safety, and reusability of high-power rockets.

In this project, the recovery system design incorporates these principles by employing a rip-stop nylon parachute with appropriately sized shroud lines, integrated with an ejection system that synchronizes with the solid fuel motor's burn profile and apogee detection. This ensures that the rocket descends safely at a controlled velocity, maximizing the potential for reuse and minimizing risk. The compatibility of the recovery system with the propulsion and structural components was a

critical design consideration, ensuring seamless integration and operational reliability.

2.4 Simulation Tools and Performance Prediction

The design and development of high-power rockets heavily rely on accurate simulation tools to predict flight performance and ensure structural integrity prior to fabrication and launch. In this project, OpenRocket and Open Motors were the primary simulation platforms used to guide the design process, validate choices, and optimize performance parameters.

OpenRocket is an open-source model rocket simulation software widely used in amateur and educational rocketry projects. It allows for comprehensive aerodynamic modeling, trajectory prediction, and stability analysis of rocket designs. The software integrates essential physical parameters such as drag coefficients, center of gravity (CG), center of pressure (CP), motor thrust curves, and mass distribution to simulate flight behavior under various atmospheric conditions. Its ability to quickly iterate different design variants made it an invaluable tool in this project, especially considering the evolving design requirements and the need to balance aerodynamic efficiency with structural constraints.

OpenRocket's aerodynamic calculations use a combination of empirical methods and analytical models, such as Barrowman equations for stability and drag predictions, which have been validated by multiple experimental studies. For instance, the Barrowman method is recognized in literature (Barrowman, 1967) for providing reliable estimates of rocket stability and aerodynamic forces, which align well with real flight data when used within its validity range.

Complementing OpenRocket, Open Motors served as the propulsion simulation tool, providing detailed thrust profiles and impulse calculations for the motor selection. Open Motors offers access to a database of commercial and custom rocket motors with associated thrust-time curves, enabling accurate prediction of acceleration, velocity, and altitude. This data was critical in matching the propulsion capabilities with the structural and aerodynamic design to meet the mission requirements.

Several studies highlight the effectiveness of combining these tools in amateur rocketry projects. According to research by Anderson et al. (2018), the integration of simulation platforms like OpenRocket and motor thrust analysis tools significantly reduces design iteration cycles, improves flight prediction accuracy, and enhances safety margins. Furthermore, the ability to model different motor configurations and simulate multiple separation events within OpenRocket allowed the project team to refine recovery systems and staging concepts early in the design phase.

The use of these simulation tools also facilitated sensitivity analyses on key design variables such as fin size, nosecone shape, and motor thrust, which helped identify optimal configurations to maximize altitude and stability. Given the limitations of physical prototyping resources, these digital tools provided a cost-effective and low-risk environment to validate design decisions before committing to fabrication.

OpenRocket and Open Motors played a crucial role in this project's design cycle, enabling

informed decision-making based on reliable performance predictions. Their use reflects a growing trend in amateur and educational rocketry to adopt accessible, validated simulation software to bridge theoretical design and practical application, thereby increasing the success rates of high-power rocket launches.

During the design and development of this high-power rocket, various software tools and expert resources played a crucial role in ensuring the accuracy, efficiency, and success of the project. SolidWorks was chosen as the primary CAD software due to its robust parametric modeling capabilities and engineering precision. It allowed us to build detailed 3D models of the rocket's structural components, simulate assembly, and perform preliminary interference checks. This step was essential for visualizing complex geometries and refining design dimensions before physical fabrication, thus minimizing costly errors.

To complement the technical CAD models, Blender was utilized to enhance the aesthetic and conceptual aspects of the rocket design. Blender's advanced sculpting, texturing, and rendering features enabled us to create high-fidelity visualizations and animations. This artistic approach provided a better understanding of the rocket's form and appearance, which is valuable for presentations, stakeholder communication, and overall design validation.

In addition to these software tools, Richard Nakka's Experimental Rocketry Web Site served as an indispensable knowledge base throughout the project. This website offers comprehensive insights into solid rocket motor design, including propellant chemistry, grain geometry, nozzle optimization, and static test analysis. Leveraging this resource helped us ground our theoretical calculations in practical experience and guided our approach to propulsion design and static testing. The detailed data and experimental results presented by Richard Nakka allowed us to benchmark our results and improve the reliability of our rocket motor's performance predictions.

Together, these tools and resources formed a critical backbone of our workflow, bridging the gap between theoretical design, practical fabrication, and visual conceptualization, thereby enhancing both the technical and creative dimensions of our project.

CHAPTER 3: Objectives

3.1 Development of a High-Altitude Rocket Using Kraft Phenolic Composite

The primary objective of this project is to design and build a sounding rocket capable of reaching an altitude of approximately 1,000 meters (1 kilometer). Achieving this target altitude requires an integrated approach that balances aerodynamic efficiency, structural integrity, and propulsion performance. A critical focus of the design is the use of kraft phenolic composite material for the rocket's structural components. This material was chosen due to its advantageous properties such as high strength-to-weight ratio, thermal resistance, and cost-effectiveness compared to conventional aerospace materials like carbon fiber or metallic alloys.

By utilizing kraft phenolic composite, the project aims to demonstrate that high-performance rocket structures can be fabricated using more accessible, sustainable materials without compromising reliability. The composite's favorable mechanical characteristics are expected to provide adequate stiffness and durability under the dynamic loads experienced during launch, ascent, and recovery. Additionally, the material's thermal stability will help withstand the heat generated by the solid fuel motor and aerodynamic heating during flight.

The design objective extends beyond structural considerations to encompass the integration of a solid fuel propulsion system made from a homemade potassium nitrate and glucose propellant. This fuels system must be compatible with the overall rocket design, ensuring stable thrust generation and reliable motor casing integration within the composite airframe. Moreover, the rocket will incorporate a functional recovery system with an ejection mechanism to deploy parachutes at apogee, safeguarding the vehicle for potential reuse and minimizing impact damage.

This objective encapsulates the development of a prototype that not only meets altitude and stability requirements but also validates the practical application of kraft phenolic composites in amateur and educational rocketry. Ultimately, this project seeks to contribute to the knowledge base on alternative composite materials in rocketry and establish a replicable process for building reliable, cost-efficient high-power rockets.

3.2 Development of a Single-Use, Modular KNO_3 -Glucose Solid Propellant Grain System

The objective of this phase is to design and implement a modular solid-fuel propulsion system using a KNO_3 -glucose mixture as the working propellant. While the module is designed for single-

use, its construction follows a modular approach—allowing the entire fuel assembly to be prepared, integrated, and later replaced as one complete unit. This balances the practical need for reusability in structure with the chemical and safety limitations of solid propellant-based systems.

The KNO_3 -glucose composition is selected for its proven reliability in amateur rocketry. It offers a stable burn profile, relatively low combustion temperature compared to composite propellants, and is manufacturable with accessible equipment and materials. The grain is cast or pressed into a pre-defined cavity—usually cylindrical with a central core—to control surface area and burn duration.

The modularity lies in how the fuel grain, nozzle, and containment structure are fabricated as a single, pre-packaged unit. This unit is inserted into the rocket during assembly and fully removed post-launch, making way for a freshly prepared module. Although the fuel itself is not reusable, this method significantly simplifies ground preparation and increases consistency between launches.

Additionally, this system is engineered to be compatible with the rocket's ejection system. The burn duration and thrust curve are matched with the required apogee timing and delay settings, ensuring the recovery sequence is initiated correctly. By integrating the propellant design into the broader mission architecture, this objective enhances overall mission reliability, while maintaining flexibility for future upgrades or changes to the grain design.

3.3 Integration of an Ejection-Based Recovery and Payload Deployment System

One of the key objectives of this project is to design a reliable, self-contained recovery system that activates upon the complete burnout of the solid fuel charge. The rocket employs a delay and ejection charge mechanism, integrated directly into the fuel casket module, to initiate recovery procedures without the need for external electronics or separate triggering mechanisms.

This system operates on a simple yet effective principle. After the main KNO_3 -glucose propellant completes its burn, a pre-packed delay composition continues to burn for a predetermined period—calculated based on the rocket's expected time to apogee using simulation tools like OpenRocket. Following the delay, the combustion of the ejection charge rapidly builds pressure within the motor casing, forcing out the nose cone.

Attached to the nose cone is one end of a ripstop nylon parachute, while the other end remains tethered to the main body using a high-strength elastic shock cord. This ensures that the parachute unfurls cleanly and stabilizes the rocket for descent. The force of the ejection is calibrated precisely to eject the nose and deploy the parachute without causing damage to the structure.

In addition to stabilizing the descent, this system is also designed to deploy any onboard payloads housed in the forward section of the rocket. The payload bay is located just beneath the nose cone, and the ejection sequence ensures both the payload and the recovery system are released simul-

taneously in a controlled manner.

This method reduces the complexity and cost typically associated with electronic deployment systems, while still achieving timely, altitude-appropriate deployment. By tightly integrating the ejection system with the propellant module, the recovery process remains synchronized with the flight dynamics, improving safety, reusability of the main structure, and mission success rate.

3.4 Validate Performance Through Simulation and Ground Testing

To ensure the rocket performs reliably and meets its design goals, its flight characteristics and subsystems are validated through both digital simulation and physical ground testing. The first step in this validation process involves using OpenRocket, an open-source rocketry simulation tool. This software allows for detailed modeling of the rocket, including its geometry, mass distribution, propulsion profile, and recovery system. By entering accurate parameters such as the center of gravity, center of pressure, thrust curves, and aerodynamic profiles, OpenRocket can simulate the entire flight sequence—from launch to recovery.

The simulations provide critical data, including predicted altitude, velocity at liftoff and apogee, time to apogee, stability margins, and the optimum delay for deploying the recovery system. These insights help in making iterative design adjustments early, without wasting physical resources.

However, simulations alone aren't sufficient. After achieving satisfactory digital results, physical ground testing is performed to validate those predictions in the real world. Static burn tests of the KNO_3 -glucose propellant help assess burn time, thrust, and structural behavior under pressure. Similarly, recovery deployment tests are carried out to verify whether the parachute and ejection mechanisms function as intended—especially since the ejection charge is integrated into the fuel casket. These tests also ensure the shock cord and nose-cone ejection mechanics can withstand operational stresses. By combining simulation and ground testing, the project ensures that theoretical expectations are reinforced with real-world validation, reducing the risk of failure during actual flight and improving confidence in the rocket's performance envelope.

CHAPTER 4: Functional Requirements

The rocket designed for this project must fulfill several critical functional requirements to ensure a successful and safe flight mission. The primary objective is for the rocket to reach an approximate target altitude of 1 kilometer (about 3,280 feet) while maintaining stable, controlled flight throughout its ascent and descent phases. All subsystems—structural, mechatronic, recovery, and propulsion—must operate reliably and in harmony to achieve this goal within the constraints of low-cost construction and limited institutional resources. From a structural standpoint, the rocket must endure the mechanical loads generated during motor ignition, takeoff, and the entire duration of flight. The frame, built using a laminated fiber-composite material based on kraft paper, must maintain its structural integrity under axial thrust, aerodynamic drag, and vibrational forces without significant deformation or failure. The design also mandates two separation events during flight: the first at apogee for payload deployment, and the second for parachute release. These separations must be mechanically robust and precisely timed to avoid premature ejection or structural damage.

The mechatronics subsystem plays a pivotal role in the autonomy and intelligence of the rocket. It must accurately detect the moment of apogee—the highest point in the rocket’s flight trajectory—and trigger the deployment mechanisms accordingly. Furthermore, the onboard electronics are expected to collect and transmit live telemetry data back to a ground station in real time, providing insight into parameters such as altitude, velocity, acceleration, orientation, and system health. This data is vital not only for performance evaluation but also for triggering critical events in-flight. The payload deployment system is required to function precisely at apogee. Its success is contingent on both the mechanical reliability of the deployment mechanism and the accuracy of the sensor readings used to determine flight position. A failure in this sequence could result in the payload being damaged or lost, defeating one of the mission’s core objectives.

For safe recovery, the rocket must deploy a parachute at a point in the descent phase that allows sufficient time for full inflation and controlled deceleration. The descent velocity must be kept within a range that avoids structural damage upon landing, allowing for inspection, possible reuse, and post-flight data retrieval. Timing, altitude, and orientation at the moment of deployment are all critical factors to be accounted for in the parachute system design. Lastly, the propulsion system must be powerful enough to carry the combined mass of the rocket and payload to the desired altitude. The motor and its housing must withstand the thermal and mechanical stresses generated during combustion. Since the rocket is intended to reach approximately 1 km, the thrust must be calibrated to achieve this target with acceptable margin while ensuring that acceleration does not destabilize the structure or compromise component integrity. The propellant choice, burn rate, and thrust profile must align with the aerodynamic characteristics of the overall design to deliver predictable and safe performance.

In summary, each subsystem of the rocket must satisfy its individual performance criteria while

integrating seamlessly into the larger framework. The collective goal is a coordinated, successful flight reaching approximately 1 km altitude, demonstrating that even unconventional, low-cost materials can deliver high-performance aerospace results when paired with thoughtful engineering and robust design practices.

CHAPTER 5: Design Approach

The design methodology adopted in this project was highly iterative and adaptive, shaped by the unique constraints and the novelty of the undertaking within our academic environment. Given that this was among the first high-power rocketry projects initiated at Anna University Regional Campus, Madurai, there was no established legacy or design precedent to follow. Consequently, we began from first principles, leveraging simulation tools such as OpenRocket for aerodynamic modeling and OpenMotor for propulsion estimation and motor behavior prediction.

Our goal was to engineer a structurally sound rocket composed of a low-cost kraft-paper-based composite material (hereafter referred to as cellulose-reinforced laminate) that could reach approximately 1,000 meters in altitude. From the outset, we prioritized simplicity in design to allow for quick iterations and easy integration of changes during development. OpenRocket enabled us to rapidly evaluate various design configurations, allowing us to refine aerodynamic features such as the nose cone profile, fin placement, and center-of-mass/stability margin with each version. The real-time visual and numerical feedback from the software helped reduce trial-and-error in physical prototyping.

One of the primary aspects of our approach was the integration of a dual-deployment mechanism. We structured the rocket to perform two separation events: one at apogee for the deployment of a drogue parachute and payload, and another during descent to deploy the main parachute. These events were synchronized with onboard sensors capable of detecting flight events, and the timing was fine-tuned using software simulations before hardware fabrication.

The payload bay design evolved through several revisions as we evaluated different positions relative to the avionics bay and main body. Initial iterations, which considered locating the payload aft of the electronics bay, proved problematic due to interference with clean deployment. Later models addressed these issues by relocating and redesigning the payload interface for reliable operation.

$$\sigma_{hoop} = \frac{Pr}{t} \quad (\text{Hoop Stress}) \quad (5.1)$$

Another vital component of our methodology was the thermal assessment of the propulsion system. Initially, we explored the idea of developing a student-researched and designed propulsion unit (SRAD). However, due to the complexities and safety concerns of propellant synthesis—especially given our limited facilities and regulatory constraints—we opted for a commercial off-the-shelf motor. OpenMotor was employed to simulate motor burn characteristics and verify that the selected motor could safely operate within the thermal tolerance limits of our composite body material. We also ensured that any thermal energy dissipated during burn did not compromise the structural integrity of the cellulose-reinforced laminate. Given the constraints in scheduling and access to advanced fabrication tools, our team prioritized modularity in assembly. Each rocket component—fins, body tube, avionics

bay, and nose cone—was designed to be individually testable and replaceable. This modular design approach allowed us to proceed with testing even when certain parts were delayed due to material availability or machining schedules.

$$\sigma_{long} = \frac{Pr}{2t} \quad (\text{Longitudinal Stress}) \quad (5.2)$$

We did not set full-scale launch as an initial success metric. Instead, we defined the successful outcome of the project as the completion of a functional prototype along with verified ground-level subsystem tests. Tests included recovery system activation, structural load tests, and electronic signal verification. These formed the foundation for future iterative improvements and gave us confidence that a full-scale launch would be achievable in subsequent project phases or by future student teams.

$$\sigma_b = \frac{My}{I} \quad (\text{Bending Stress}) \quad (5.3)$$

$$\sigma_v = \sqrt{\sigma_x^2 - \sigma_x\sigma_y + \sigma_y^2 + 3\tau_{xy}^2} \quad (\text{Von Mises Stress}) \quad (5.4)$$

The design journey was not without risks. Dependencies between subsystems occasionally caused bottlenecks, particularly when design finalization of one component hinged on the completion of another. Additionally, due to our reliance on workshop facilities for manufacturing, delays in training and access often impacted our timeline. These were mitigated through parallel tasking, improved documentation, and maintaining multiple design options in simulation until fabrication could be initiated.

$$\text{FOS} = \frac{\sigma_{yield}}{\sigma_{max}} \quad (\text{Factor of Safety}) \quad (5.5)$$

By combining structured simulation-based analysis with hands-on fabrication planning, our design approach provided a realistic pathway for realizing a student-led high-power rocket capable of reaching significant altitudes using sustainable, cost-effective materials.

5.1 Aerodynamics and Structures

The aerodynamic and structural design of the rocket plays a vital role in achieving stable and efficient flight. Each component was selected and engineered to balance performance, manufacturability, and structural integrity while adhering to the constraints of available materials and fabrication techniques. Computational simulations and prior references were used to optimize the shape, weight,

and placement of components to ensure minimized drag, sufficient stability, and controlled descent.

$$\text{Static Margin} = \frac{CP - CG}{D} \quad (\text{in calibers}) \quad (5.6)$$

$$F_d = \frac{1}{2}\rho V^2 C_d A \quad (\text{Drag Force}) \quad (5.7)$$

$$Re = \frac{\rho V L}{\mu} \quad (\text{Reynolds Number}) \quad (5.8)$$

5.1.1 Nose Cone

The nose cone serves as the foremost aerodynamic structure of the rocket and plays a critical role in minimizing drag during ascent. In early stages of the design, various nose cone geometries such as conical, hemispherical, and parabolic were evaluated using OpenRocket simulations to analyze their impact on aerodynamic performance. While hemispherical cones offer better internal volume and are often used in low-speed model rockets, they produce significantly more drag. Conical shapes are easier to fabricate and provide moderate drag reduction, but are not optimal for higher-speed applications. Parabolic cones offer the least drag at transonic speeds but are complex to model and manufacture.

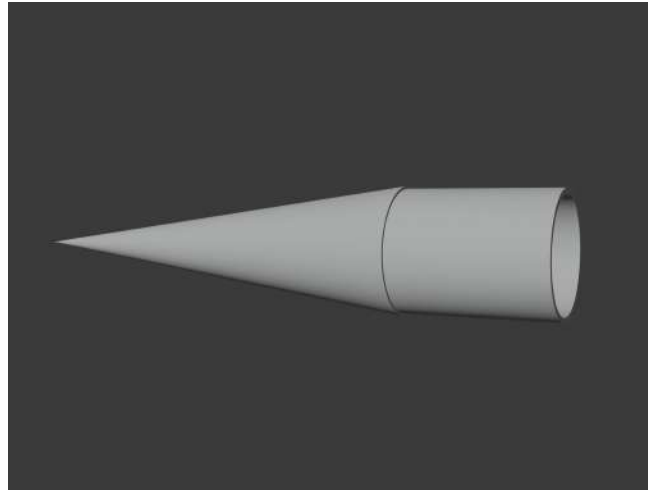


Figure 5.1: Nose Cone Concet model from Blender

Ultimately, the long conical shape was selected due to its favorable drag characteristics and structural compatibility with the body tube and coupler assembly. Simulations run in OpenRocket showed that the ogive profile maintained stability across various flight conditions, especially under the thrust profile expected from the custom potassium nitrate-glucose based solid fuel. The smooth curvature of the ogive cone facilitates a streamlined airflow, significantly reducing form drag as the rocket climbs through the atmosphere.

Nose cone shape: Conical

Shape parameter: 0.0

Length: 28.6 cm

Base diameter: 7.87 cm

☐ Automatic

Wall thickness: 0.318 cm

☐ Filled

☐ Flip to tail cone

A conical nose cone has a profile of a triangle.

Material

Component material: Kraft phenolic (0.95 g/cm³)

Component finish: Regular paint (60 µm) Set for all

Figure 5.2: Nose Cone Data from Open Rocket

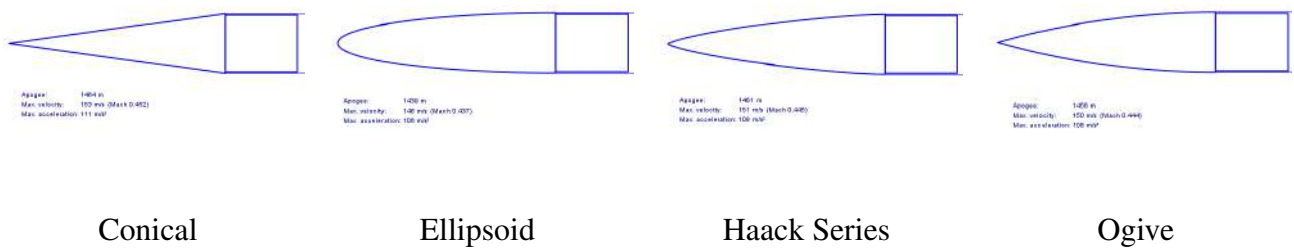


Figure 5.3: Comparison of Four Nose Cone Shapes

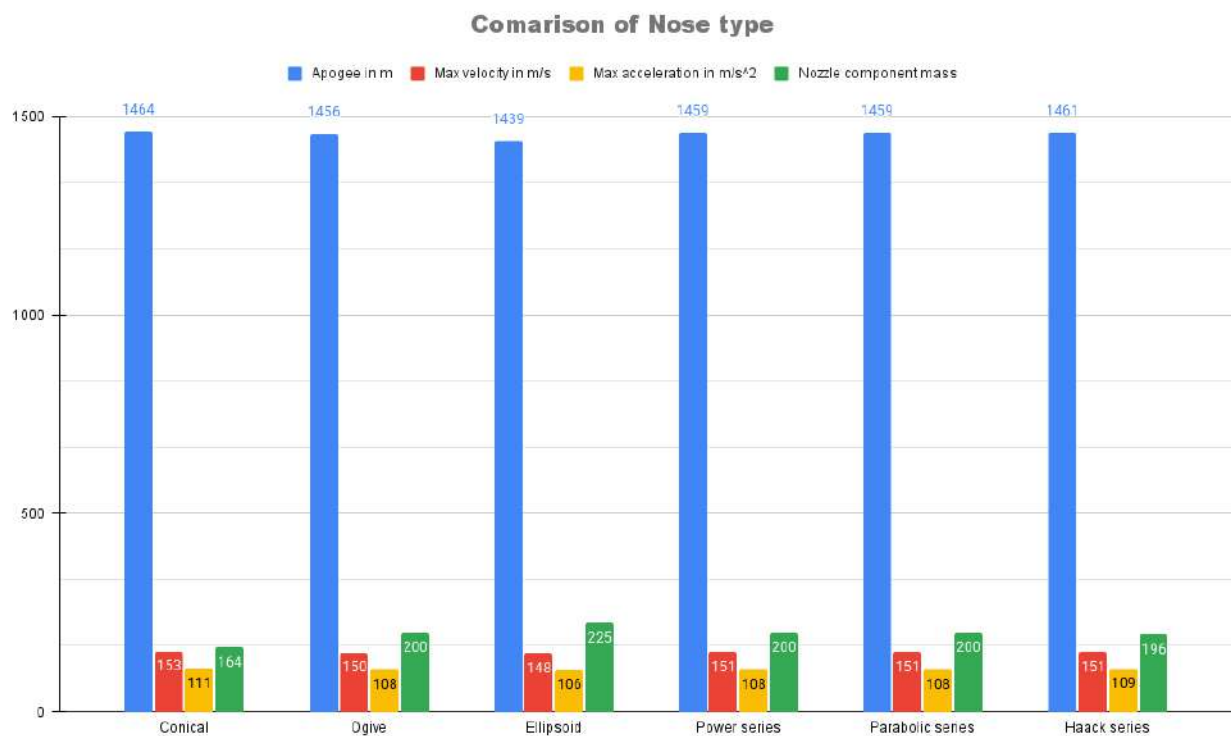


Figure 5.4: Nose cone comparison

The selected nose cone has a length of 28.6 cm and is fabricated from kraft phenolic composite for its light weight and structural integrity. The design process focused heavily on compatibility; the nose cone integrates seamlessly with the kraft phenolic body tube using an internal coupler system. This structural continuity ensures the overall rocket maintains aerodynamic efficiency while also being simple to assemble and disassemble for payload access or recovery system installation.

5.1.2 Fins

For the aerodynamic stabilization of the rocket during flight, a set of four clipped delta fins was selected and integrated into the design. The decision followed a detailed examination of existing fin configurations commonly used in high-power amateur and student rocketry, particularly those suitable for subsonic to low-supersonic velocities. Studies consistently highlighted the clipped delta shape as an optimal choice for balancing drag reduction, structural strength, and ease of fabrication. The clipped

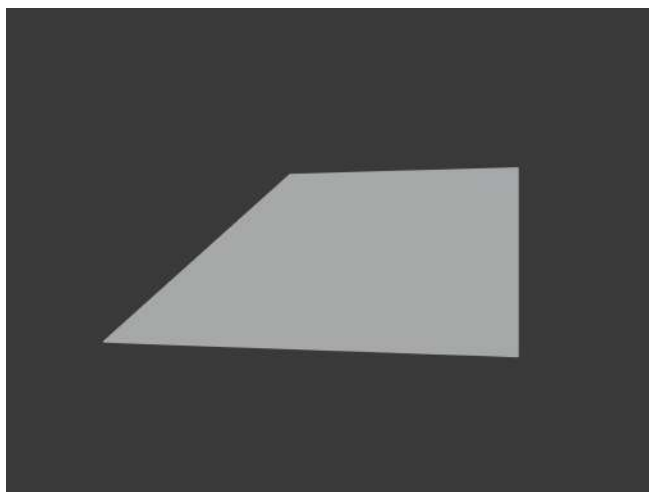


Figure 5.5: Fin Concept model from Blender

delta fin design, which combines the performance advantages of swept delta fins with reduced base drag, was particularly well-suited for our flight profile. Our simulations in OpenRocket confirmed that the configuration ensured the center of pressure remained at a stable distance behind the center of gravity—approximately 7 cm aft, giving a static margin of 0.806 calibers (or 4.24% of the body diameter), which maintained stable flight without being excessively overstable.

The trapezoidal airfoil profile was selected to simplify manufacturing and ensure consistent bonding to the kraft phenolic composite airframe. This airfoil form offers modest aerodynamic performance while remaining forgiving in terms of alignment and fabrication tolerances. The material used for the fins is the same kraft phenolic composite as the body tube, providing a consistent structural behavior under thermal and mechanical loads during flight. Each fin is permanently bonded to the airframe using high-strength epoxy. While detachable fins were considered during early design phases, they were ultimately set aside in favor of permanence for increased reliability and lower structural complexity. This approach was also advised by experienced mentors, especially given the use of a homemade propulsion system.

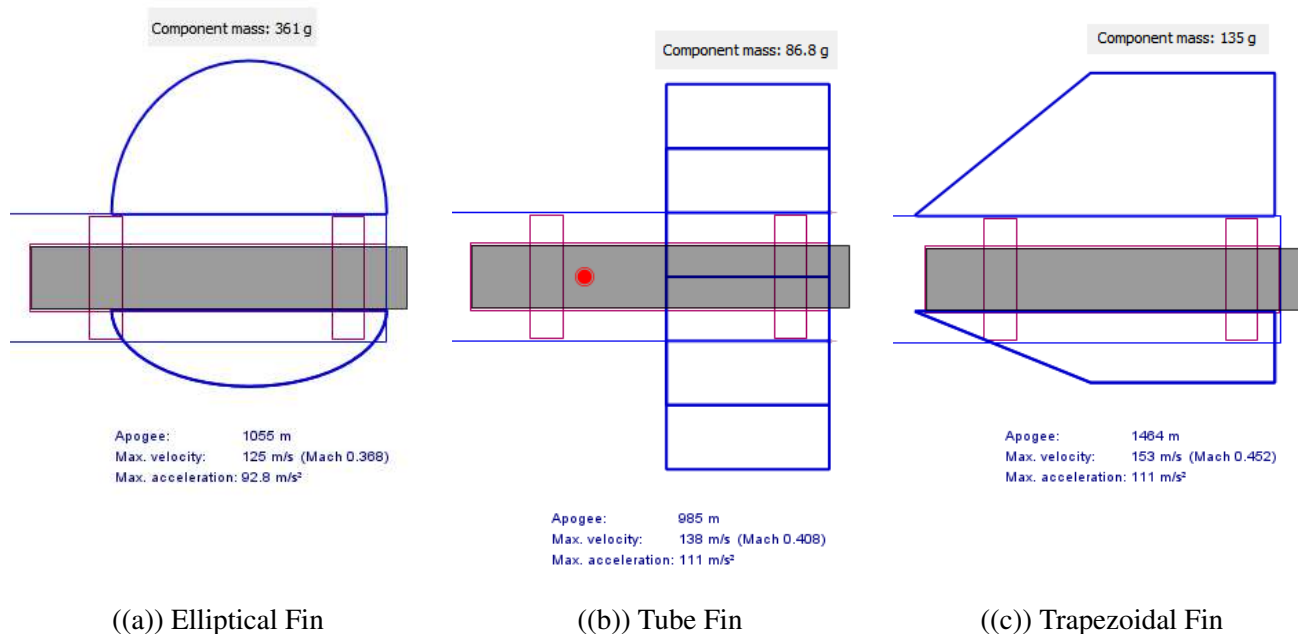


Figure 5.6: Different Fin Designs

Figure 5.7 shows the configuration options for a fin set in the Open Rocket software:

- Number of fins:** 3
- Fin cant:** 0°
- Fin cross section:** Rounded
- Thickness:** 0.318 cm
- Placement:**
 - Position relative to: Top of the parent component
 - plus 63.8 cm
 - Fin rotation: 0°
- Material:**
 - Component material: Kraft phenolic (0.95 g/cm³)
 - Component finish: Regular paint (60 μm) [Set for all]
- Root Fillets:**
 - Fillet radius: 0 cm
 - Fillet material: Cardboard (0.68 g/cm³)

Figure 5.7: Fin Set data from Open Rocket

5.1.3 Couplers

The couplers in our rocket serve as critical structural connectors between modular sections of the body tube, providing both mechanical strength and functional integration for recovery and avionics systems. We adopted an internal coupler design made from kraft phenolic composite, optimized for its balance of stiffness, low mass, and seamless internal profile. This design ensures efficient transmis-

sion of aerodynamic and inertial loads while preserving the interior space for components such as the ejection charge, parachute rigging, and electronics bay.

Each coupler is designed with an extended shoulder length of approximately one body diameter (15.67 cm), which enhances axial alignment and increases joint stiffness—particularly useful during high-speed ascent and recovery deployment phases. The fit between the coupler and body tube was finely tuned to achieve a snug, interference-free connection, eliminating the need for mechanical fasteners such as shear pins. This allowed us to retain clean internal aerodynamics and reduce stress concentrations typically caused by traditional hardware. The main avionics coupler also functions as

The screenshot displays the 'Component name: Tube coupler' in the Open Rocket software. The 'Custom' tab is selected, and the 'Parts Library' button is visible. The 'General' tab is active, showing the following parameters:

- Length: 15.2 cm (with a slider)
- Outer diameter: 7.62 cm (with a slider)
- ☐ Automatic
- Inner diameter: 7.44 cm (with a slider)
- Wall thickness: 0.089 cm (with a slider)

The 'Placement' section shows 'Position relative to: Top of the parent component' and 'plus 18.1 cm' (with a slider). The 'Material' section shows 'Component material: Kraft phenolic (0.95 g/cm³)'.

Figure 5.8: Coupler data from Open Rocket

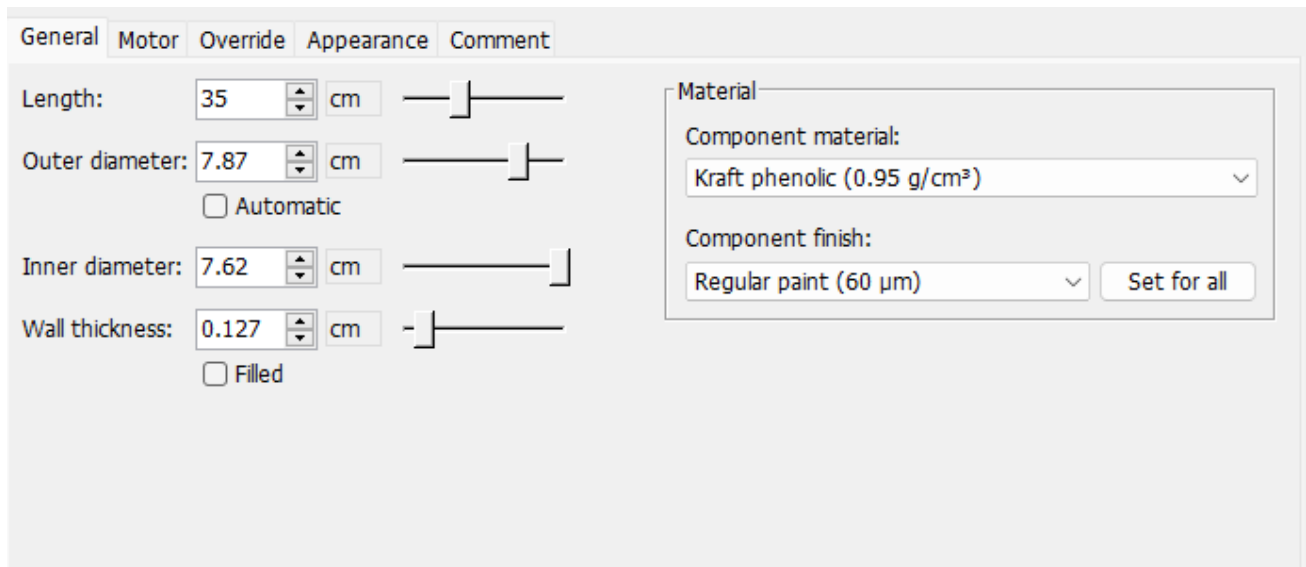
a deployment joint for the recovery system, utilizing a custom-fitted ejection charge cavity integrated directly into the fuel casket. This design uses the pressure pulse from the KNO_3 –glucose solid propellant’s end-burn phase to push the nose cone and eject the parachute in a reliable and consistent manner. The coupler system was validated through ground-fit testing and simulations to ensure that it can withstand both the longitudinal and hoop stresses without deformation or failure.

By using kraft phenolic instead of fiberglass or metallic materials, the coupler maintains excellent strength-to-weight characteristics while remaining thermally stable, easy to bond with epoxy, and cost-effective for amateur rocketry. Additionally, its compatibility with RF signals enables future integration of onboard telemetry systems without the need for external antennas.

5.1.4 Body

The body of the rocket forms its primary structural framework, enclosing and supporting all critical internal systems including the propulsion module, recovery mechanism, and any onboard payload. Designed to endure aerodynamic loads, motor-induced stresses, and recovery-phase shock, the body must balance mechanical strength with minimal mass. For this reason, kraft phenolic composite—reinforced with an epoxy matrix—was selected as the material of construction. With a density of

approximately 0.95 g/cm^3 , this material offers a favorable strength-to-weight ratio, ease of manufacturing, and better reparability compared to conventional options like carbon fiber, which, while lighter in some configurations, involves greater cost and complexity in fabrication.



General Motor Override Appearance Comment

Length: 35 cm

Outer diameter: 7.87 cm

☐ Automatic

Inner diameter: 7.62 cm

Wall thickness: 0.127 cm

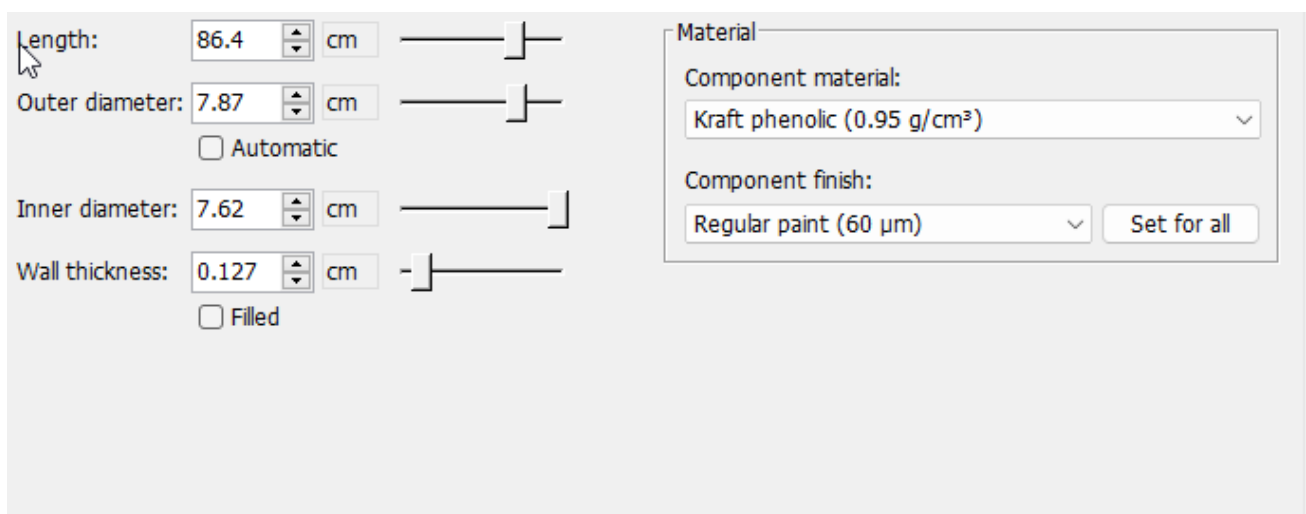
☐ Filled

Material

Component material: Kraft phenolic (0.95 g/cm^3)

Component finish: Regular paint ($60 \mu\text{m}$) Set for all

Figure 5.9: First Body data from Open Rocket



Length: 86.4 cm

Outer diameter: 7.87 cm

☐ Automatic

Inner diameter: 7.62 cm

Wall thickness: 0.127 cm

☐ Filled

Material

Component material: Kraft phenolic (0.95 g/cm^3)

Component finish: Regular paint ($60 \mu\text{m}$) Set for all

Figure 5.10: Second Body data from Open Rocket

The structural configuration comprises two cylindrical segments: one measuring 80 cm in length for housing the propulsion system, and another 75 cm in length designated for the recovery assembly and payload integration. Both segments share a uniform outer diameter of 15.67 cm and an inner diameter of 14.8 cm, ensuring seamless integration with couplers and internal bulkheads. These dimensions were finalized through iterative modeling and stability analysis in OpenRocket, taking into account the position of the center of gravity and center of pressure to ensure stable subsonic flight.

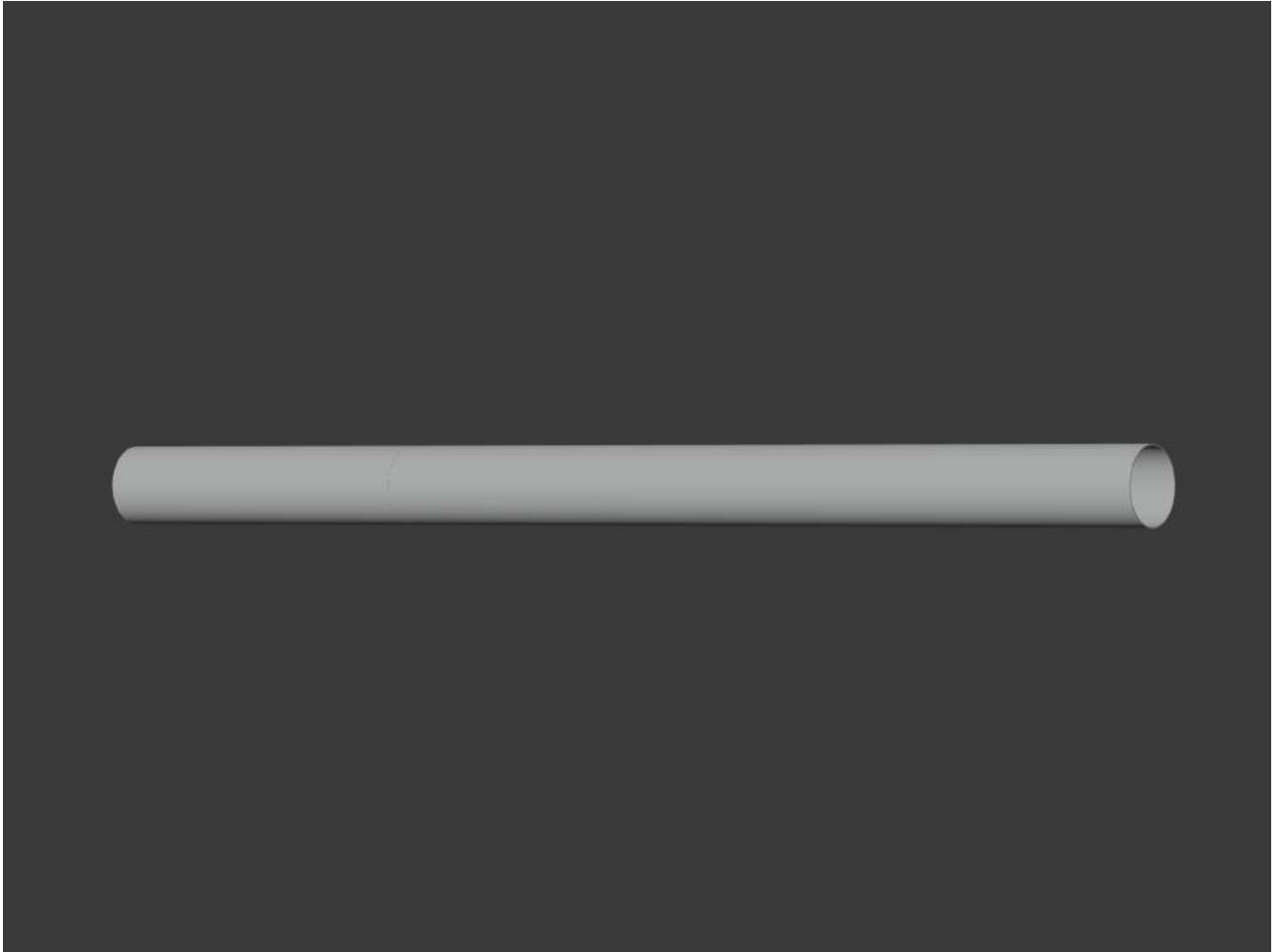


Figure 5.11: Body Concept model from blender

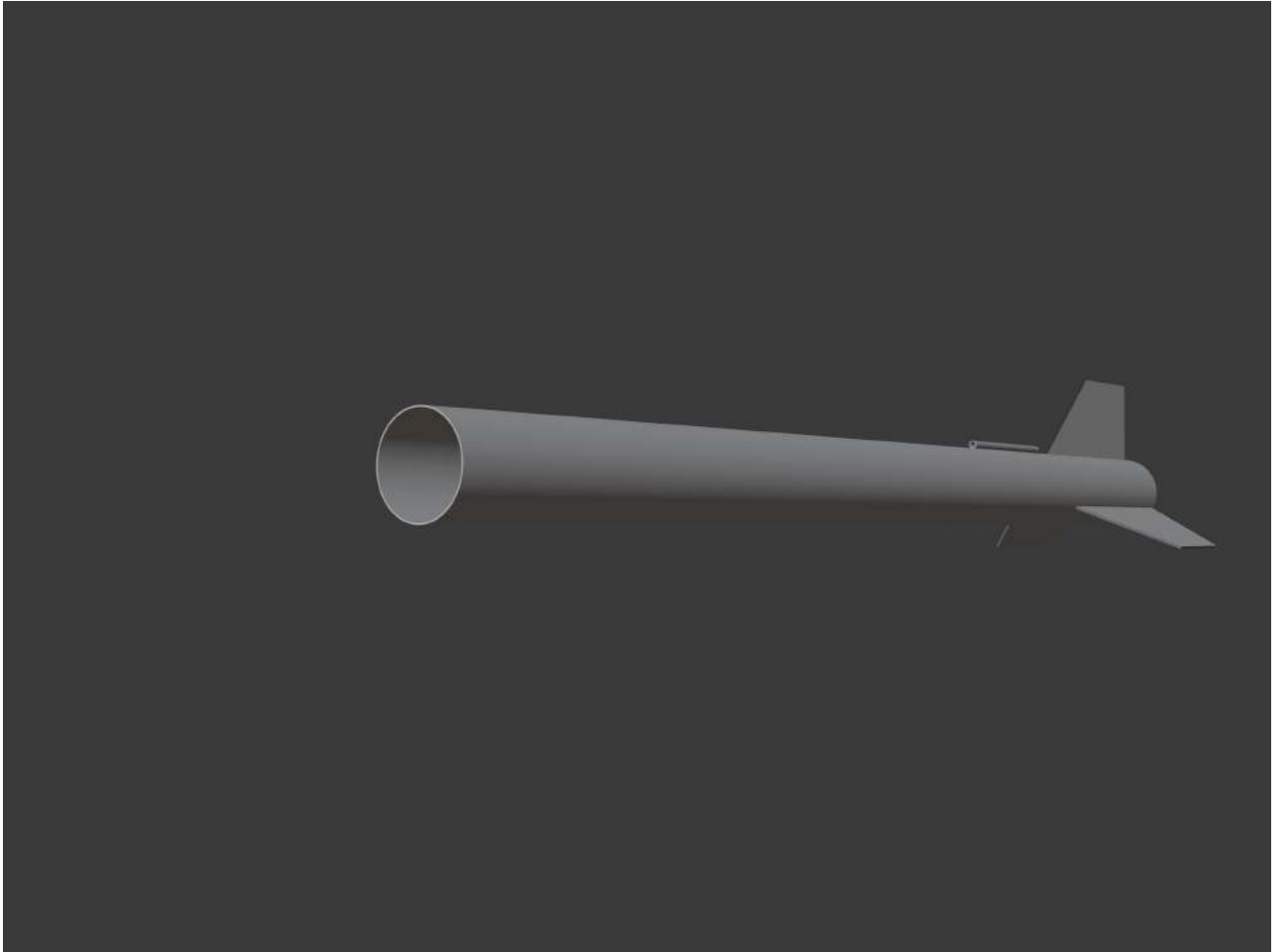


Figure 5.12: Body with fins concept model from blender

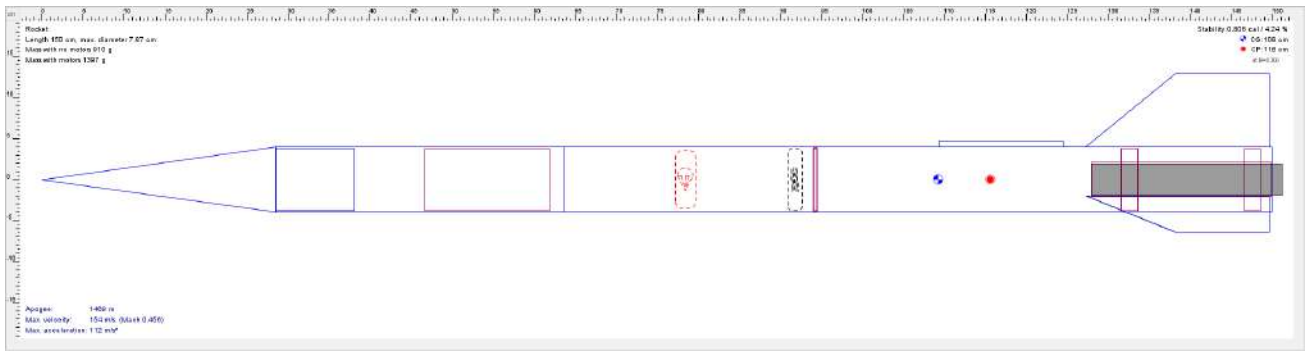


Figure 5.13: Rocket data from open rocket

The cylindrical form factor was reinforced by an external wrapping of fiberglass cloth impregnated with epoxy, significantly enhancing axial and hoop strength without adding unnecessary mass. This configuration also accommodates internal pressure variations and localized thermal effects generated by the combustion process and ejection charge. Additionally, the chosen material and dimensions allow sufficient electromagnetic transparency for future avionics and telemetry modules, making the structure not only robust but also compatible with data systems necessary for performance validation.

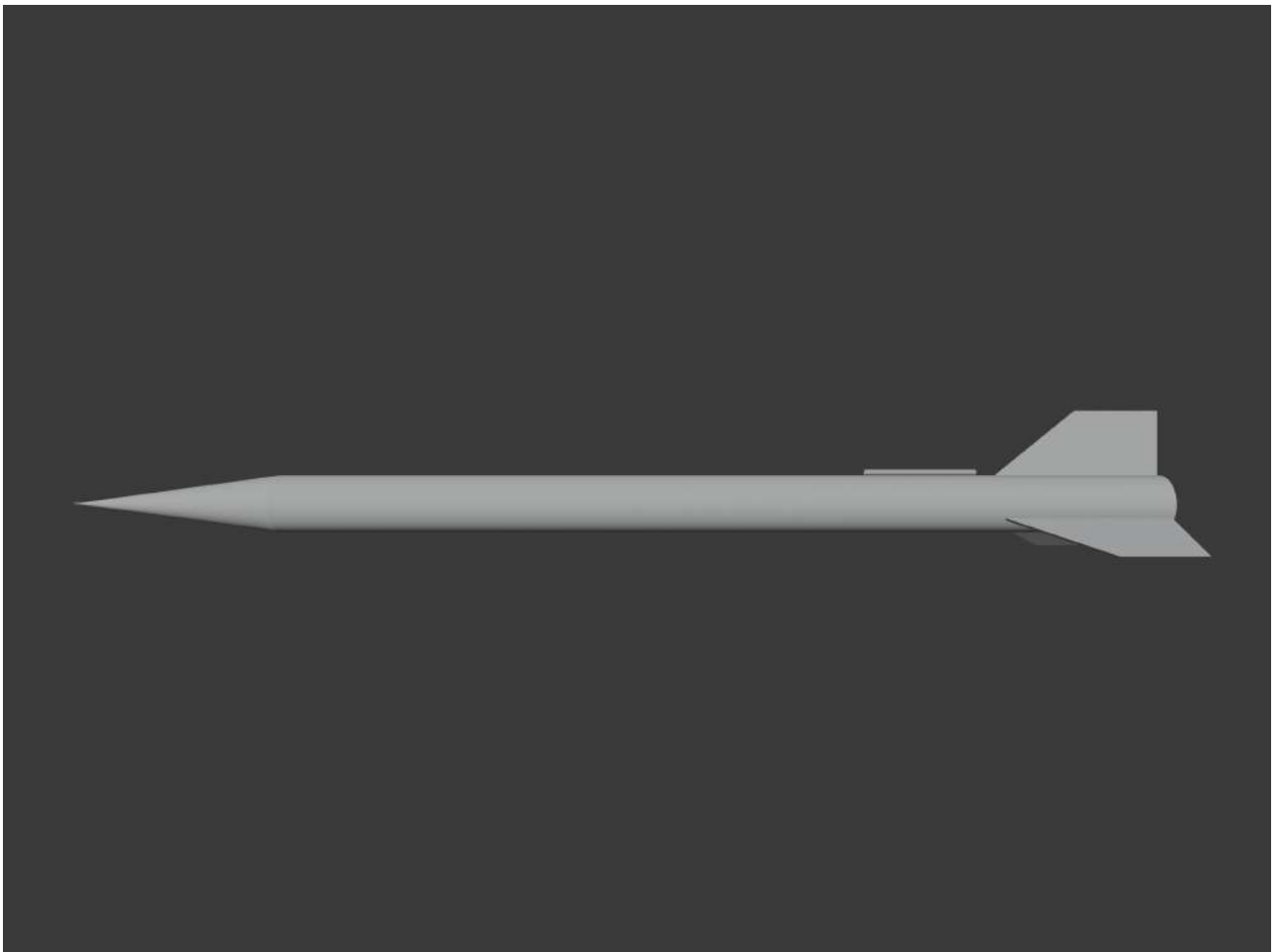


Figure 5.14: Full rocket Concept model from blender

Nozzle Design

beta degrees Nozzle convergence half-angle
alpha degrees Nozzle divergence half-angle

Dc 38 mm Chamber inside diameter
Dt 13.41 mm Nozzle throat diameter
De 37.93 mm Nozzle exit diameter

Lc 17.56 mm Convergence length
Ld 57.68 mm Divergence length
Lo 75.24 mm Overall length

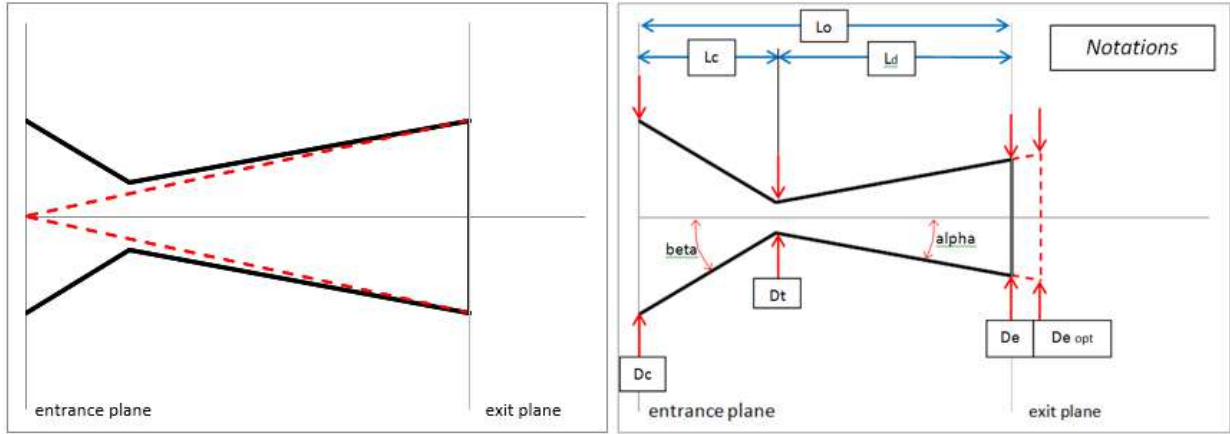


Figure 5.15: Nozzle data

5.1.5 Nozzle Design

The nozzle is a crucial component in the rocket's propulsion system, responsible for converting the high-pressure, high-temperature combustion gases into a high-speed exhaust jet, thereby producing thrust according to Newton's third law. In this project, a fixed-geometry converging-diverging (CD) nozzle, commonly known as a de Laval nozzle, was used. The nozzle is designed to be compatible with the characteristics of the KNO_3 -sugar solid propellant and is fabricated using a heat-resistant epoxy-clay composite to withstand thermal and mechanical stresses.

The primary parameters considered in the nozzle design include the throat diameter, exit diameter, expansion ratio, and material selection. The throat diameter was chosen based on an iterative balance between chamber pressure, burn rate of the propellant, and desired thrust. The exit diameter was optimized for near-atmospheric conditions to maximize exhaust velocity. The design process involves applying the following key formulae:

$$F = \dot{m}v_e + (p_e - p_a)A_e \quad (\text{Thrust equation})$$

$$v_e = \sqrt{\frac{2\gamma}{\gamma - 1} \cdot RT_c \cdot \left(1 - \left(\frac{p_e}{p_c}\right)^{\frac{\gamma-1}{\gamma}}\right)} \quad (\text{Exhaust velocity})$$

$$A_t = \frac{\dot{m}}{p_c} \cdot \sqrt{\frac{RT_c}{\gamma}} \cdot \left(\frac{2}{\gamma + 1} \right)^{\frac{\gamma+1}{2(\gamma-1)}} \quad (\text{Throat area})$$

$$\epsilon = \frac{A_e}{A_t} \quad (\text{Nozzle expansion ratio})$$

Where:

- F is the thrust (N)
- \dot{m} is the mass flow rate (kg/s)
- v_e is the exhaust velocity (m/s)
- p_e, p_a are the exit and atmospheric pressures respectively (Pa)
- A_e, A_t are the exit and throat areas respectively (m²)
- γ is the specific heat ratio of the exhaust gases (typically 1.2–1.3 for sugar propellant)
- R is the specific gas constant (J/kg·K)
- T_c is the chamber temperature (K)
- p_c is the chamber pressure (Pa)

The nozzle was 3D-printed initially for prototype validation and later fabricated using a molded composite of clay and high-temperature epoxy for the final build. The converging section smoothly guides the gas toward the throat, minimizing flow separation. The diverging section expands the gases to supersonic speeds, increasing the specific impulse. A small graphite insert was added to the throat region to prolong its life during the burn.

By carefully matching the nozzle's geometry to the combustion characteristics of the propellant, a stable and efficient thrust profile was achieved. The final nozzle geometry ensures that the thrust-to-weight ratio exceeds the required minimum for lift-off and contributes to the rocket's peak altitude performance.

Common name:	I59
Total impulse:	487 Ns (52% I)
Avg. thrust:	59.5 N
Max. thrust:	172 N
Burn time:	8.15 s
Launch mass:	487 g
Empty mass:	215 g
Motor type:	Reloadable

Figure 5.16: Motor Characteristic

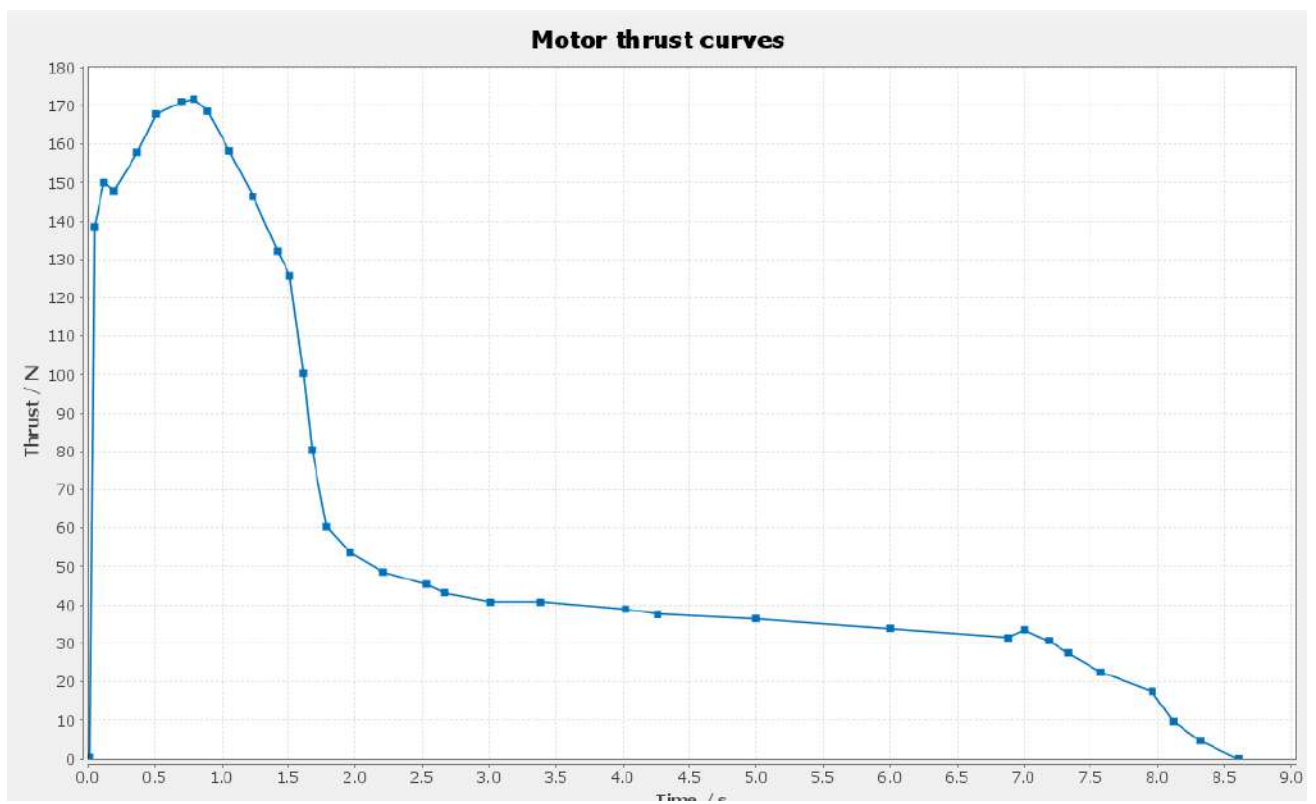


Figure 5.17: Motor Characteristic from open motor

CHAPTER 6: Mechatronics and Controls

6.1 Electronics

The electronics system in this rocket serves as the central intelligence hub, responsible for sensing, logging, interpreting, and commanding critical flight events. Given the low-cost, self-fabricated nature of this vehicle, the electronics suite was designed with modularity, reliability, and functional redundancy in mind. The entire avionics unit is housed within a dedicated payload bay, safely enclosed and isolated from the motor compartment using kraft phenolic bulkheads and couplers.

At the heart of the system is a microcontroller-based flight computer that interfaces with multiple onboard sensors. These sensors record atmospheric pressure, acceleration, temperature, and altitude in real time. A barometric pressure sensor, paired with an inertial measurement unit (IMU), enables accurate apogee detection through data fusion, reducing false positives due to rapid velocity changes or transient spikes in altitude.

The system architecture supports dual deployment logic—triggering the ejection charges for both drogue and main parachutes. The first charge is fired immediately after apogee is detected, using a small delay charge integrated into the fuel module itself, which pushes the nose cone forward and initiates deployment. The second charge is altitude-dependent and is either handled by the same controller with preset thresholds or, in redundant configurations, by a secondary system triggered via a barometric cutoff. Both igniter circuits are electrically isolated and powered by independent voltage regulators to ensure fail-safe operation.

To ensure data reliability and mission traceability, all flight data is logged to onboard storage—typically a microSD module—and simultaneously transmitted over RF telemetry to a ground station. This dual strategy ensures recovery of flight logs even in case of telemetry failure. The entire system is powered by a compact, rechargeable Li-ion battery pack secured within the avionics bay and protected against overcurrent events.

While advanced commercial systems offer higher resolution and integration, our custom-built avionics emphasize affordability, adaptability, and repairability. The structure allows easy swaps of controller boards, sensor modules, or telemetry units depending on mission profile or component failure—making the electronics bay as modular and scalable as the rest of the vehicle architecture.

6.2 Aviation Bay

The avionics bay is designed as a compact, cylindrical payload module that integrates all critical electronics, including flight computers, sensors, telemetry, and power systems. Built from kraft

phenolic tubing reinforced for structural stability, the bay is mounted between two circular phenolic bulkheads and reinforced using three stainless steel threaded rods. These rods serve as both the structural spine of the bay and mounting points for internal components, ensuring rigidity and shock resistance throughout flight.

A vertical mounting plate made of lightweight fiberboard or 3D-printed polymer is fixed perpendicular to the rods. This plate supports the central flight computer, barometric pressure sensors, IMU, GPS module, and additional telemetry units. The layout is designed for quick access during ground testing and simplifies future upgrades or module replacements.

Power is supplied by a bank of rechargeable Li-ion batteries securely placed within foam cutouts, positioned to balance the load and maintain CG stability. This configuration also minimizes vibration-induced wear and ensures electrical safety during ignition and ejection events.

The cylindrical shape of the bay not only complements the rocket's aerodynamic profile but also supports even pressure distribution, minimizing localized stress points. It allows for optimal airflow within the airframe and helps protect delicate electronics from excessive heat and shock during motor ignition and parachute ejection events.

Internally, careful attention has been given to wire routing, isolation of high-current paths (e.g., e-matches), and physical separation of telemetry and sensor wiring to avoid interference. The modular design allows the avionics bay to be removed independently of the coupler or payload sections, easing field servicing and post-flight data retrieval.

This structure, while simple, offers robust performance under the dynamic forces of launch, separation, and recovery, ensuring reliable operation of all electronic subsystems throughout the flight.

6.3 Parachute Deployment

The parachute deployment system is a critical safety mechanism designed to enable controlled descent and recovery of the rocket's main components — the nose cone and body — after motor burnout and apogee. Our system uses a dual-stage ejection process consisting of a delay charge followed by an ejection charge, both initiated electrically through the onboard avionics.

$$M = \sum mr^2 \quad (\text{Moment of Inertia}) \quad (6.1)$$

Upon motor burnout, the delay charge is ignited, producing a timed interval allowing the rocket to reach apogee and stabilize. After this delay, the ejection charge activates, generating a rapid build-up of pressure inside a sealed compartment between the nose cone and the rocket body. This pressure forces the nose cone to separate cleanly from the main body, deploying the parachute stored within the body tube. The design ensures that while the nose cone detaches to allow airflow and parachute deployment, it remains tethered to the main rocket body via the parachute shroud lines. This

tethered configuration guarantees that both sections descend together, reducing the risk of damage from uncontrolled impacts.

$$KE = \frac{1}{2}mv^2 \quad (\text{Kinetic Energy}) \quad (6.2)$$

$$q = \frac{1}{2}\rho V^2 \quad (\text{Dynamic Pressure}) \quad (6.3)$$

The mechanical coupling between the nose and body is achieved through a retention interface designed to hold firmly during ascent but release reliably under the force generated by the ejection charge. This interface often consists of a shoulder or groove machined into the nose cone base and body tube, ensuring a secure yet releasable joint.

6.4 Theoretical and Practical Analysis

The separation and recovery mechanism of the rocket relies on creating a sufficient pressure differential inside a sealed compartment between the nose cone and the forward body tube. This pressure is generated by igniting a pre-measured charge of black powder, which rapidly produces expanding gases. The black powder mass was calculated using the ideal gas law to ensure that the internal pressure reaches approximately 30 psi—enough to overcome the frictional and mechanical resistance of the nose cone without damaging the airframe or avionics bay.

$$F = ma \quad (\text{Newton's Second Law}) \quad (6.4)$$

$$s = ut + \frac{1}{2}at^2 \quad (\text{Displacement}) \quad (6.5)$$

The ignition method is passive and relies on a time-delay fuse embedded into the motor casing. This fuse is ignited by the residual heat of the motor's combustion and is timed to burn through and ignite the black powder after a delay corresponding to the rocket's predicted apogee. This ensures parachute deployment occurs only after the rocket slows near the top of its trajectory, preventing premature ejection under high velocity.

$$h_{max} = \frac{v^2}{2g} \quad (\text{Maximum Altitude}) \quad (6.6)$$

The ejection charge is housed in a central cavity behind the nose cone and sealed with a light barrier that retains the powder until ignition. Upon ignition, the rapid gas expansion generates a force sufficient to eject the nose cone and deploy the parachute. The parachute system includes a ripstop nylon canopy, elastic shock cord, and nylon shroud lines designed to minimize shock loads on deployment.

$$t_{apogee} = \frac{v}{g} \quad (\text{Time to Apogee}) \quad (6.7)$$

This mechanical timing system, although simple, proved effective for our single-stage rocket

flight profile, eliminating the need for onboard electronics and minimizing points of failure.

6.5 Parachute Material and Design

We selected ripstop nylon for the parachute material due to its ideal balance of tensile strength, weight, and durability. The ripstop weave incorporates reinforced threads at regular intervals, which provide excellent tear resistance, critical in the high-stress environment of rapid parachute deployment. Its low density reduces overall payload weight while maintaining structural integrity.

Parachute sizing is derived through energy balance and drag equations, targeting a terminal descent velocity of approximately 3 m/s to prevent impact damage upon landing. The drogue parachute is sized smaller to reduce drift and stabilize the rocket's descent, while the main parachute provides the majority of the drag force during landing.

The shroud lines of the parachute are attached securely to the rocket body at one end and to the base of the nose cone at the other, allowing both parts to descend together while minimizing oscillations or tangling. This tethering also ensures the nose cone does not become a hazardous projectile post-separation.

6.6 System Integration and Safety Considerations

The entire ejection system is integrated into the avionics bay, with redundancies to safeguard against ignition failure or premature deployment. The electronics control both charges, with fail-safe programming and real-time data logging for post-flight analysis.

The sealed volume containing the black powder charge is designed to contain combustion gases and direct the ejection force axially, minimizing lateral forces that could damage the airframe. Additionally, all materials exposed to combustion byproducts are chosen for thermal resistance and minimal outgassing.

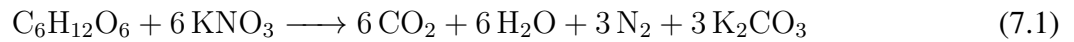
Due to supply constraints, 3FG black powder was utilized instead of 4FG. Although 4FG offers a faster and smoother burn, 3FG's combustion characteristics were successfully compensated for by adjusting the charge mass and optimizing the ignition timing.

CHAPTER 7: Propulsion

The propulsion system of our rocket is based on a sugar-based solid propellant using Potassium Nitrate KNO_3 as the oxidizer and Glucose as the fuel. This class of propellant is widely used in amateur rocketry due to its relatively simple manufacturing process, availability of materials, and safe handling characteristics compared to composite propellants.

The fuel was prepared by finely grinding both KNO_3 and glucose into powder form to ensure uniform particle distribution. These powders were mixed in a weight ratio of approximately 65:35 and then slowly heated over a temperature-controlled hot plate. As the glucose melted (around 146°C), it began to encapsulate the KNO_3 particles, forming a thick slurry. Heating was carefully maintained below 160°C to avoid thermal decomposition or auto-ignition. Once a uniform, caramel-like consistency was achieved, the hot mixture was poured into cylindrical molds lined with insulation material and allowed to cool and solidify, forming a single fuel grain.

Upon ignition, this propellant undergoes a redox reaction, producing large volumes of hot gases. A simplified combustion reaction is given below:



The combustion generates high-temperature gases such as carbon dioxide, water vapor, and nitrogen, along with potassium carbonate in the solid phase. The pressure developed from this gas expansion inside the combustion chamber is the primary source of thrust. The gas is expelled through a nozzle, which converts thermal and pressure energy into kinetic energy, thus propelling the rocket upward according to Newton's Third Law of Motion.

The propellant's performance is characterized by its burn rate and specific impulse. The burn rate is dependent on the internal chamber pressure and follows a power-law relationship, expressed as:

$$r = aP^n \quad (7.2)$$

Here, r is the linear burn rate, P is the chamber pressure, a is a proportionality constant, and n is the pressure exponent. For sugar-based propellants, the pressure exponent typically ranges between 0.3 and 0.5. The internal grain design and nozzle diameter were chosen to ensure the chamber pressure remains within the optimal range for steady combustion.

The total impulse generated by the propellant is related to the mass of the propellant and its specific impulse (I_{sp}). Specific impulse is a measure of the efficiency of the propellant and is defined by:

Basic Data and Kn Calculation

Title: Example Rocket Motor (L-Class)
utilizing KNDX propellant.

Motor chamber:

Dc 38 mm Chamber diameter (inside)
Lc 232.0 mm Chamber length (inside)
Vc 263115 mm³ Chamber volume (empty)

Propellant grain:

Propellant type KNSU select

Do 38.00 mm Outer diameter (initial)
do 5 mm Core diameter (initial)
Lo 220.00 mm Segment length (initial)
N 1 Number of segments

Outer surface: Inhibited select

Core surface: Exposed select

Ends surface: Inhibited select

Lgo 220 mm Grain length (initial)

Vg 245186 mm³ Grain volume (initial)

Vt 0.932 Volumetric loading fraction

ρ' grain 1.889 g/cm³ Grain ideal density

0.95 Density ratio (actual/ideal)

ρ grain 1.795 g/cm³ Grain actual density

m grain 0.440 kg Grain mass (initial)

Abeo 0 mm² End burning area (initial)

Abco 3456 mm² Core burning area (initial)

Abso 0 mm² Outer surface burning area (initial)

Abo 3456 mm² Total burning area (initial)

Target MEOP: 900 psi select Maximum chamber pressure (target)

Kn max: 264 Ratio of Burning area / throat area (max)

Nozzle: Ato 141 mm² Throat cross-section area (initial)

Dto 13.411 mm Throat diameter (initial)

Dtf 13.41 mm Throat diameter (final)

Kn max	264
Kn min	24
Kn avg	144

Figure 7.1: KN calculation

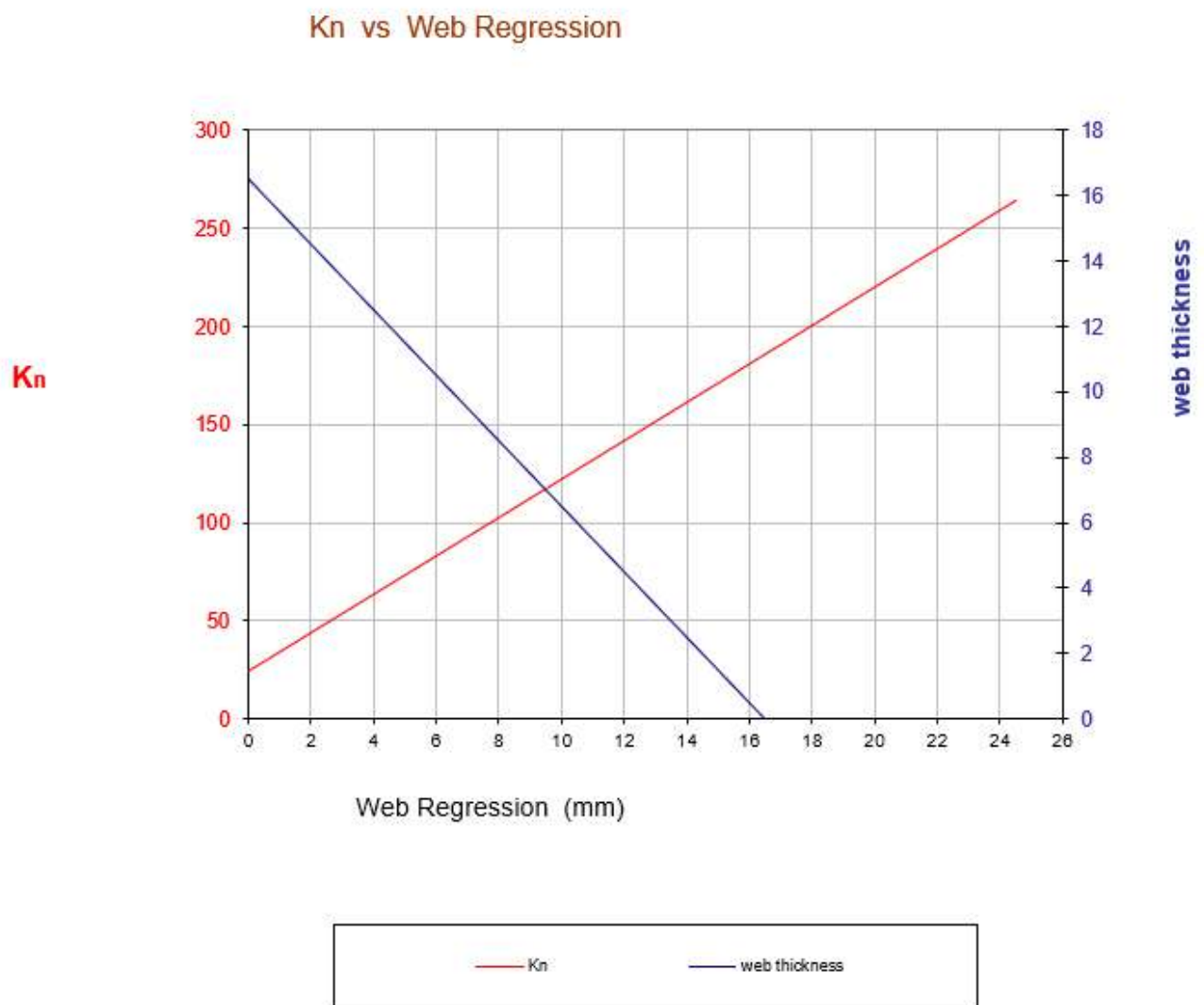


Figure 7.2: K_n vs Web regression

$$I_{sp} = \frac{F_{thrust}}{\dot{m}g_0} \quad (7.3)$$

Where F_{thrust} is the average thrust, \dot{m} is the mass flow rate of the expelled gases, and g_0 is the standard acceleration due to gravity. For the current propellant, the expected specific impulse ranges from 115 to 130 seconds under sea-level conditions.

The solidified grain was cast into a single cylindrical cavity with a central bore to allow internal burning (end-burner or BATES design). This geometry ensures consistent regression and maintains thrust over the burn duration. The combustion chamber is constructed using a kraft phenolic composite body, selected for its high-temperature tolerance, low weight, and resistance to internal pressure and thermal erosion.

$$I_t = \int_0^{t_b} F(t) dt \quad \text{(Total Impulse)} \quad (7.4)$$

$$F_{avg} = \frac{I_t}{t_b} \quad \text{(Average Thrust)} \quad (7.5)$$

$$\dot{m} = \frac{m_{propellant}}{t_b} \quad \text{(Mass Flow Rate)} \quad (7.6)$$

$$T/W = \frac{F_{max}}{mg} \quad \text{(Thrust-to-Weight Ratio)} \quad (7.7)$$

Ignition is initiated using a nichrome wire that heats upon current application, igniting a small booster charge placed in contact with the main propellant grain. The resulting combustion rapidly builds pressure and begins the primary burn phase.

The exhaust nozzle, designed with a convergent-divergent profile, helps expand the gases and accelerates them to supersonic velocities, thus generating the required thrust. Nozzle erosion is minimized by using a graphite insert in the throat region. The nozzle dimensions were derived based on the expected chamber pressure and desired exit velocity using the isentropic flow relations for compressible gas expansion. This propulsion system offers a low-cost, efficient, and relatively safe solution for high-power rocketry. The use of sugar-based propellant provides adequate thrust to meet our target altitude and flight profile while allowing full control over the burn rate and geometry through fabrication techniques.

CHAPTER 8: Methodology

The methodology adopted for the development of the high-power model rocket was centered around a balance between theoretical analysis, material experimentation, and iterative prototyping. The project began with extensive research into lightweight structural materials that could withstand the thermal and mechanical stresses generated during launch. Kraft paper laminated with epoxy resin was selected as the primary construction material for the airframe, fins, and internal bulkheads due to its low cost, ease of manufacturing, and favorable strength-to-weight ratio. The phenolic-composite approach allowed the rocket to maintain rigidity while remaining lightweight enough for optimal thrust-to-weight performance.

The propulsion system was based on a sugar-based solid propellant composed of potassium nitrate (KNO_3) and glucose. This mixture, commonly referred to as a “Rocket candy” propellant, was prepared by carefully heating the oxidizer and fuel in a controlled environment to initiate partial caramelization and achieve a homogeneous melt. The hot slurry was poured into a kraft-based paper motor casing designed to resist internal pressure buildup. The burn characteristics of the propellant were modeled theoretically to estimate the total impulse and thrust curve, assuming complete combustion and ideal nozzle flow. The primary driving mechanism for thrust was the generation of high-temperature gases and pressure buildup in the combustion chamber, which expelled through a converging-diverging nozzle to produce thrust based on Newton’s third law. The relationship between thrust (F), mass flow rate (\dot{m}), and exhaust velocity (v_e) was given by:

$$F = \dot{m}v_e + (p_e - p_a)A_e \quad (8.1)$$

where p_e is the exhaust pressure, p_a is ambient pressure, and A_e is the nozzle exit area. The effective pressure generated from the combustion of the KNO_3 -glucose mixture was carefully calculated to match the structural limits of the kraft phenolic body tube.

The recovery system relied on a dual-phase parachute deployment mechanism using a delay charge followed by an ejection charge. At apogee, a small quantity of black powder was ignited to pressurize the avionics bay and eject the nose cone. One end of the parachute was attached to the separated nose section, while the other end remained tethered to the rocket body, ensuring both parts descended safely and symmetrically. The charge mass was determined using the ideal gas law, modified to estimate the necessary pressure to overcome coupler friction:

$$PV = nRT \quad \Rightarrow \quad m = \frac{PVM}{RT} \quad (8.2)$$

where P is the required pressure, V is the volume between the bulkhead and piston, M is the

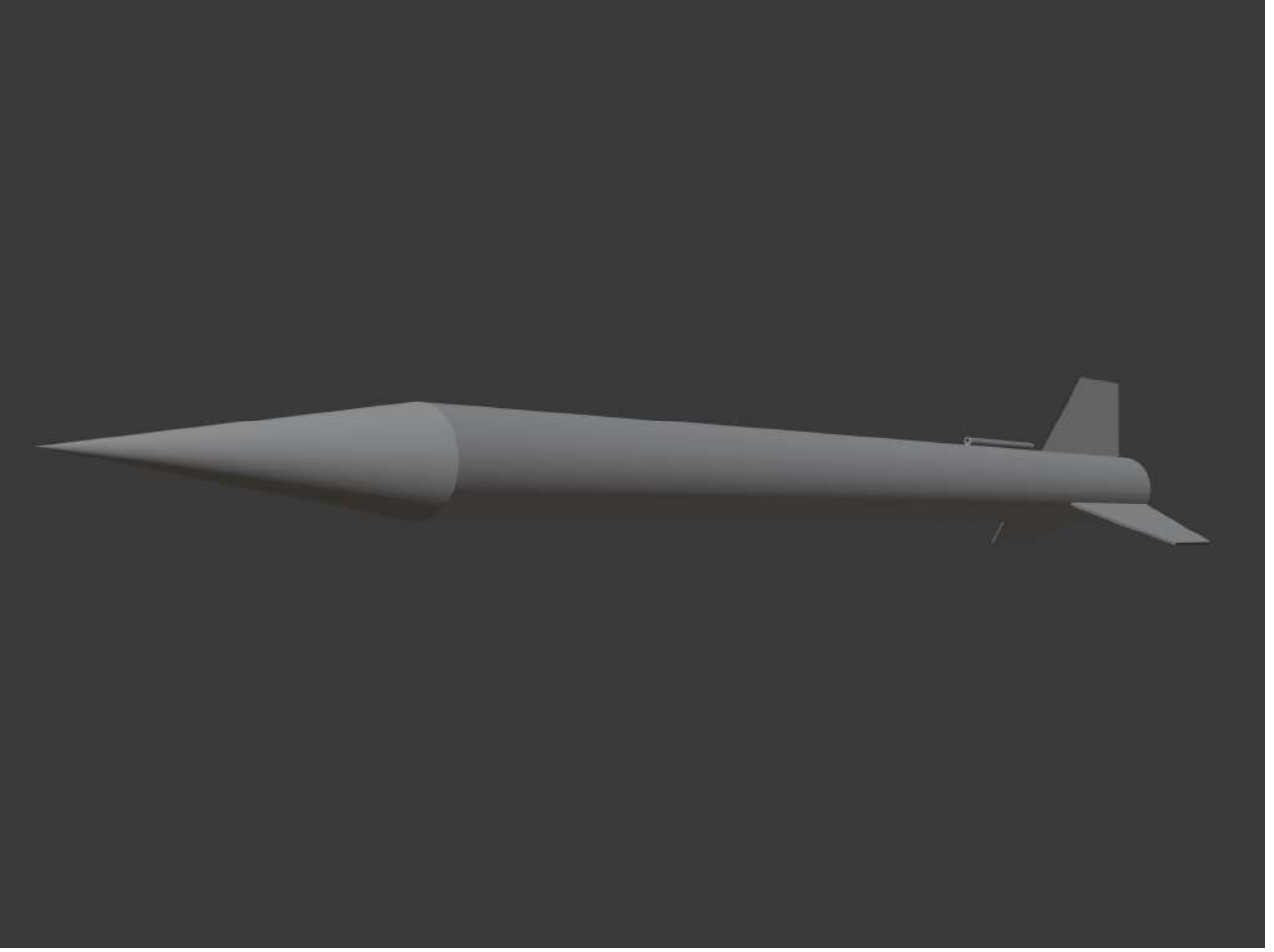


Figure 8.1: Conept Model from blender

molar mass of the gas, R is the gas constant, and T is the combustion temperature. Based on this, approximately 1.6 grams of black powder was used for reliable separation. The avionics system was assembled within a cylindrical bay using three threaded rods for structural rigidity. A custom PCB was mounted vertically for optimal space utilization, and sensors including barometers, accelerometers, and GPS modules were installed for telemetry and apogee detection. Power was supplied via high-performance lithium cells securely positioned along the inner wall of the bay. All software logic for flight monitoring and deployment control was pre-programmed into the microcontroller before integration.

$$q = -k \frac{dT}{dx} \quad (\text{Fourier's Law of Heat Conduction}) \quad (8.3)$$

$$q = \epsilon \sigma T^4 \quad (\text{Radiative Heat Flux}) \quad (8.4)$$

The final configuration was validated through multiple OpenRocket simulations to predict flight stability, apogee, and descent characteristics. Ground tests were conducted to verify structural performance, separation reliability, and burn behavior of the propellant under static conditions. With all systems cross-validated against theoretical expectations, the rocket was cleared for flight trials under controlled launch conditions.

8.1 Prototype

The development of a physical prototype was a crucial phase in validating the aerodynamic, structural, and systems integration aspects of the rocket. Serving as both a proof of concept and a learning tool, the prototype demonstrated the feasibility of the proposed design and enabled the team to test key functionalities of subsystems including structural joints, parachute separation, fin alignment, and material selection. More importantly, it allowed for the evaluation of manufacturing accuracy and inter-team coordination across integrated parts.



Figure 8.2: Rocket Art from Blender

The prototype construction involved the fabrication and assembly of the rocket's major structural components: the nose cone, body tube, fins, and couplers. These components were produced using a combination of kraft phenolic composite materials, fiberglass tubes, and epoxy bonding. The selection of materials was guided by the need for low weight, sufficient mechanical strength, and RF transparency, particularly for ensuring proper telemetry signal propagation. Structural joints were fixed using high-strength epoxy to eliminate the stress concentrations and failure points that are common with mechanical fasteners. The coupling sections and body tube were joined with precision tolerances to ensure aerodynamic smoothness and load distribution during flight.

The constructed prototype closely mirrored the final flight design in terms of dimensions and materials, with only minor exceptions such as the use of fiberglass couplers and commercial phenolic tubes for body structure. These were incorporated to ensure high dimensional precision where critical alignment and sealing were necessary. Through physical testing and visual inspection, the prototype highlighted several practical concerns, such as potential misalignments at joints, epoxy curing inconsistencies, and tolerances that required refinement. These findings were documented to inform



Figure 8.3: Rocket Concept art from open rocket

adjustments in the final design and assembly procedure. Overall, the prototype served its intended role effectively by bridging the gap between digital design and physical realization. It enabled early detection of design flaws, improved confidence in structural durability, and validated the team’s capacity for precision manufacturing and system-level integration, thereby laying a robust foundation for the final flight model.

8.1.1 Manufacturing and Fabrication

Nose cone

A key innovation in our rocket’s construction was the development of a custom composite material used for fabricating the nose cone. This material was created by combining layers of kraft paper with a carefully formulated epoxy resin. The objective was to achieve a material that exhibits high strength-to-weight ratio, structural rigidity, and aerodynamic smoothness—characteristics traditionally associated with glass or carbon fiber composites, but at a significantly lower cost.

The manufacturing process began by cutting kraft paper into long, narrow strips, which were then impregnated with a low-viscosity epoxy resin. This resin was chosen for its deep penetration capability and strong adhesive bonding once cured. Each resin-soaked strip was wound around a rotating conical mandrel to form the nose cone’s shape. The winding was done with care to maintain consistent tension and avoid air bubbles between the layers, ensuring uniform thickness and strength throughout the structure.

As the layers accumulated, the resin began to gel and hold the form, gradually forming a rigid shell. The part was then allowed to cure at ambient temperature for several hours, followed by a post-curing phase under moderate heat to enhance cross-linking within the epoxy matrix. Over time, the



Figure 8.4: Nose

composite hardened into a structure that closely mimicked the mechanical behavior of traditional fiber-reinforced materials. This behavior has been supported in literature that shows kraft paper, when fully saturated with epoxy and layered strategically, achieves performance metrics comparable to early-generation composite laminates, particularly in applications involving moderate structural loads and aerodynamic shaping.

Once cured, the nose cone was carefully sanded and finished to improve its aerodynamic profile and ensure a smooth surface finish. The final result was a durable, lightweight, and cost-effective composite nose cone with excellent impact resistance and dimensional stability. This method not only allowed for rapid prototyping and iterative testing but also opened the possibility of using sustainable and widely available materials in aerospace-style fabrication.

The successful implementation of this process demonstrates the viability of low-cost composite manufacturing using kraft paper and epoxy, especially in educational and experimental rocketry where budget and material access are constrained. This approach also aligns with existing research in sustainable composites, where lignocellulosic fibers and paper-based materials are gaining attention as viable alternatives to synthetic fibers in low-to-medium performance applications.

Body

The main body of the rocket was constructed using a kraft paper-based phenolic composite that we custom-fabricated to achieve a high strength-to-weight ratio while maintaining a cost-effective and accessible manufacturing process. The fundamental goal behind this approach was to replicate the properties of traditional phenolic and fiberglass tubing using readily available materials and minimal tooling, while ensuring the body maintained structural rigidity under aerodynamic and internal pressure loads.

To begin fabrication, a rotating mandrel setup was assembled to serve as a support for the body tube during the lay-up and curing phases. This involved using a steel pipe with a diameter smaller than the intended internal diameter of the body tube. Circular end plates were crafted from plywood and precisely sanded to match both the outer diameter of the steel mandrel and the inner diameter of the kraft composite tube. Once inserted into both ends of the tube, the mandrel provided a stable axis around which the material could be wound and rotated during lamination. The core of the body tube



Figure 8.5: Body of the Prototype

structure was constructed by spirally winding strips of kraft paper that were fully impregnated with a low-viscosity epoxy resin. These strips were tightly wrapped under uniform tension along the length of the mandrel to build up the desired wall thickness. This spiral winding technique helped distribute

mechanical loads efficiently along the axis of the rocket. After a sufficient number of layers had been applied, the full layup was allowed to settle and begin curing. Excess resin that surfaced during winding was smoothed out to prevent inconsistencies and surface defects.

To enhance the composite's structural performance, a final outer layer of epoxy-saturated kraft paper was laid longitudinally, followed by wrapping the body tube with clear mylar film. This film served both to compress the laminate during curing and to create a smooth finish by squeezing out excess resin and eliminating air bubbles. This compression method is essential in resin-based composites to prevent delamination and voids that could compromise the structural integrity during launch.

The curing process occurred in two stages. Initially, the assembly was left at room temperature to allow the epoxy to gel and set. Once the structure became semi-rigid, it was post-cured under a gentle heat source to accelerate cross-linking within the resin matrix, resulting in a significantly more rigid and impact-resistant tube. Once fully cured, the body tube was demolded from the mandrel and trimmed to exact length using a precision band saw.

The final result was a lightweight, durable body tube that rivals traditional phenolic and fiberglass components in terms of performance. The kraft-phenolic composite body proved strong enough to endure flight stresses, while also being lighter and more affordable than its commercial counterparts. This method also enabled rapid prototyping and allowed for adjustments during the early development phase, which would be highly beneficial for future iterative designs.

Fins

The rocket's fins were crucial for ensuring aerodynamic stability throughout flight and were manufactured using the same kraft paper-epoxy composite method employed in the construction of the body tube. The dimensions and profile of the fins were derived directly from simulations conducted in OpenRocket software, which allowed precise modeling of the center of pressure and overall aerodynamic behavior. Based on these simulations, a three-fin configuration was selected for optimal balance between stability and drag. To fabricate the fins, multiple sheets of kraft paper were first cut into rough fin outlines, slightly oversized to allow for trimming after curing. Each layer was impregnated with a low-viscosity epoxy resin and stacked to the desired thickness, ensuring uniform resin distribution throughout the layup. The layers were pressed flat between two acrylic sheets wrapped in polyethylene to prevent adhesion, and then clamped under moderate pressure to allow the composite to cure into a rigid plate. This pressure curing method helped minimize trapped air and ensured strong interlayer bonding.

Once cured, the flat laminated sheets were removed and precisely cut into their final fin shapes using a fine-tooth band saw. Edges were sanded to achieve smooth aerodynamic profiles, with a slight bevel applied to the leading and trailing edges to reduce drag during flight. A slot-mounting configuration was chosen to provide strong mechanical engagement between the fins and the rocket body. The aft end of the body tube was pre-slotted before final curing, allowing the fin roots to be inserted directly into the wall of the tube.



Figure 8.6: Fins

Each fin was bonded into its respective slot using a high-strength epoxy adhesive. Care was taken to ensure precise angular spacing of 120 degrees between each fin, maintaining symmetry and aerodynamic consistency. After the fins were secured in place, internal fillets of thickened epoxy were applied at the root-tube junctions to enhance load distribution and prevent delamination during high-G phases of launch and recovery. Finally, external surface fillets were added for additional mechanical support and aerodynamic smoothing.

The resulting fin assembly, though constructed from lightweight materials, exhibited excellent rigidity and strength. By integrating kraft paper–epoxy laminates, we achieved a cost-effective yet structurally robust solution, comparable to commercial-grade fiberglass fins. This fabrication method also allows for easy replication or modification in future design iterations.

Fuel Container and Nozzle Fabrication

The fuel container for the propulsion system was fabricated using the same kraft paper and epoxy resin-based composite technique employed for the body and nose cone. This approach not only maintained material consistency and reduced cost, but also yielded a container that was lightweight, durable, and structurally robust. The kraft-phenolic composite provides good thermal insulation and moderate resistance to the internal pressures and thermal loads generated during combustion, making it suitable for short-duration high-impulse flights.



Figure 8.7: Motor along with the nozzle

The fuel container was cylindrical in shape, matched precisely to the grain diameter of the solid propellant. The composite layup involved rolling multiple layers of kraft paper around a metal mandrel, with each layer impregnated with epoxy resin to ensure bonding and structural integrity. After achieving the required wall thickness, the entire assembly was allowed to cure under compression to eliminate air gaps and promote resin penetration. Once cured, the container formed a rigid and stable casing for casting the sugar-based solid fuel directly inside.

Particular attention was given to the fabrication of the nozzle, as it is a critical component in maximizing thrust and directing exhaust flow. The nozzle was fabricated using the same kraft-phenolic composite material, but with reinforced bonding and additional layers at the throat and exit sections to enhance heat resistance and withstand the extreme mechanical stresses during combustion. A mold was created to form the precise shape of the nozzle, based on the principles of a de Laval nozzle design. The de Laval nozzle, characterized by its converging-diverging shape, was selected for its ability to accelerate combustion gases from subsonic to supersonic speeds, thereby maximizing the thrust output. The nozzle begins with a converging section that narrows down to a throat, where the flow reaches Mach 1 (choked flow). Following this, a diverging section allows the high-temperature, high-pressure gases to expand, converting thermal energy into kinetic energy, and accelerating the exhaust to supersonic velocities.

The de Laval nozzle's effectiveness is governed by the area ratio between the exit and throat, as well as by the combustion chamber pressure and temperature. According to rocket propulsion theory,

the ideal exit velocity v_e of the exhaust can be calculated by:

$$v_e = \sqrt{\frac{2\gamma}{\gamma - 1} \cdot \frac{RT_c}{M} \left(1 - \left(\frac{p_e}{p_c} \right)^{\frac{\gamma-1}{\gamma}} \right)}$$

Where:

- γ is the ratio of specific heats (for combustion gases, typically around 1.2–1.3),
- R is the universal gas constant,
- T_c is the combustion chamber temperature,
- M is the molar mass of the exhaust gases,
- p_c and p_e are chamber and exit pressures respectively.

Care was taken to ensure the nozzle throat diameter and expansion ratio matched the expected operating parameters for the sugar-based fuel, thereby optimizing the specific impulse and thrust coefficient. The nozzle's inner surface was treated with a thin coating of heat-resistant ceramic-like epoxy for additional thermal protection during the peak thrust phase.

This handmade composite nozzle has proven to be both lightweight and capable of handling the thermal and mechanical loads required for low-altitude solid propulsion, while demonstrating the practical viability of using affordable, accessible materials in student-led rocketry.

8.1.2 Propulsion Preparation

The propulsion system for this rocket utilized a homemade solid composite propellant based on a potassium nitrate (KNO_3) and sugar mixture, a formulation commonly known in amateur rocketry as "rocket candy." This type of propellant is classified as a composite sugar-based solid fuel and is widely documented for its simplicity, safety (compared to other high-energy propellants), and relatively high performance for low-cost propulsion systems. The oxidizer-to-fuel ratio selected for this project was 70:30 by mass, where potassium nitrate acted as the oxidizer and glucose (alternatively sucrose) as the fuel.

The preparation process was carried out in a controlled environment to ensure safety and consistency in propellant quality. The KNO_3 and glucose powders were first finely ground and sieved separately to ensure homogeneity and enhance the reactivity during the heating phase. These were then thoroughly dry-mixed in the 70:30 ratio using a stainless-steel bowl to avoid contamination and static discharge risks. A double-boiler system was used to heat the mixture gently, keeping the temperature below 150°C to prevent premature decomposition or ignition. During this phase, the mixture gradually transitioned from a dry powder into a viscous caramel-like fluid. This is the caramelization process of sugar, which allows the molten sugar to encapsulate the oxidizer particles, forming a

homogenous energetic material.

Heating was continued until the mixture took on a golden-brown appearance and reached a thick, pourable consistency—indicative of proper caramelization and integration of oxidizer within the fuel matrix. Care was taken to stir the mixture continuously to prevent local overheating, charring, or uneven distribution of oxidizer. Once the desired consistency and coloration were achieved, the hot propellant was immediately poured into pre-fabricated cylindrical fuel casings made using the kraft-phenolic composite technique. These casings provided both containment and insulation for the propellant during storage and combustion.

After casting, a central perforation was made axially along the length of the propellant grain using a metal rod while the material was still malleable. This perforation follows a core-burn geometry, enhancing the initial surface area exposed to combustion and providing a more uniform burn rate and higher thrust generation during flight. The core-burn configuration is well-documented to improve the pressure curve characteristics of sugar-based motors, as it allows the surface area to remain approximately constant throughout much of the burn cycle.

Once cooled, the solidified propellant took on a hard, glassy consistency, indicating successful curing. These fuel grains were then stored in sealed containers to prevent moisture absorption, which could degrade both the mechanical and energetic properties of the propellant.

In addition to its primary role as a combustion chamber, the fuel container also houses a delay charge and an ejection charge system essential for the rocket's recovery sequence. Positioned aft of the main propellant grain, a dedicated cavity was included during the casting process to accommodate the delay composition. This delay charge, typically made of a slower-burning mixture of oxidizer and fuel (in a reduced reactivity formulation), burns at a controlled rate after the main propellant has fully combusted. It acts as a timing mechanism, ensuring that the parachute deployment occurs only after the rocket reaches its apogee. Once the delay charge is consumed, it ignites the ejection charge—a small but energetic black powder-like mixture—that generates a rapid pressure buildup. This sudden pressure is directed toward the recovery bay, effectively ejecting the nose cone or a coupler, and pushing the parachute assembly out of the body tube. To ensure effectiveness, this mechanism was pressure-tested using sealed-end trials, and the container was structurally reinforced around the recovery bay interface with extra layers of kraft-epoxy laminate. This integration ensures that the recovery mechanism functions reliably without compromising the structural or thermal integrity of the propulsion system.

This method of propulsion preparation has been validated by several amateur rocketry groups and research papers. Studies such as those by Humble, Henry et al. ("Space Propulsion Analysis and Design") and in experimental rocketry forums and journals show that a KNO_3 -sugar ratio around 65–75% oxidizer yields optimal specific impulse (I_{sp}) values in the range of 80–120 seconds, depending on geometry and chamber pressure. While this is lower than composite AP-based motors, the ease of manufacturing and safety profile make it ideal for student-led and low-budget aerospace projects.

This propellant formulation and casting process were selected for its balance of performance, cost, and ease of handling, with rigorous attention paid to safe heating and uniform casting. These efforts contributed to the reliable operation of the propulsion system during both static and flight tests, demonstrating the effectiveness of sugar-based propellants in low-altitude high-power rocketry.

8.1.3 Parachute Deployment System

The parachute deployment system is a critical subsystem designed to ensure a safe and controlled descent of the rocket post-apogee. It is primarily based on a black powder ejection mechanism, integrated into the aft end of the solid fuel grain. The system utilizes a dual-phase approach, beginning with a delay charge followed by an ejection charge, both housed in a specialized cavity within the fuel container structure.

$$F_{drag} = \frac{1}{2}\rho V^2 C_d A \quad (\text{Parachute Drag Force}) \quad (8.5)$$

The parachute itself is fabricated from ripstop nylon, a material widely used in aerospace recovery systems due to its high tensile strength, low density, and thermal resistance. Ripstop nylon possesses a tensile strength exceeding 660 N per 5 cm² [?], and its interwoven reinforcing pattern prevents tears from propagating, ensuring durability under dynamic deployment conditions. To enhance thermal survivability during ejection, the parachute is wrapped in a heat-resistant Nomex or foil-based blanket, which shields it from the hot gases generated by the black powder charge.

$$V_t = \sqrt{\frac{2mg}{\rho C_d A}} \quad (\text{Terminal Velocity}) \quad (8.6)$$

Deployment is initiated after motor burnout, when the delay charge burns slowly over a calculated duration (based on the predicted time-to-apogee) and then ignites the ejection charge. This ejection charge—typically consisting of finely granulated black powder—burns rapidly, creating a high-pressure gas burst within the sealed recovery bay. The resultant pressure buildup acts against the coupler or bulkhead, forcing the nose cone to detach from the main airframe. The nose cone, tethered to the shock cord, drags the parachute out of its compartment. One end of the parachute is anchored to the main rocket body via a high-strength shock cord, while the other end remains attached to the detached nose cone. This ensures both sections descend together under canopy, distributing the aerodynamic load and reducing descent velocity. Such tethered separation also prevents the nose from free-falling, which could otherwise lead to damage or safety hazards. The use of an elastic shock cord—constructed from Kevlar or nylon—helps absorb deployment forces and minimize structural stress.

The deployment mechanism was designed using guidelines from existing rocketry literature and empirical models. According to Estes and Tripoli standards, the required ejection charge mass was estimated using the equation:

$$m = \frac{P \cdot V}{R \cdot T} \quad (8.7)$$



Figure 8.8: Parachute

where m is the required black powder mass, P is the target pressure (typically 25–30 psi), V is the recovery bay volume, R is the ideal gas constant, and T is the flame temperature (approx. 2100 K for black powder). Based on these parameters, approximately 1.5–2.0 g of black powder was found sufficient to achieve the necessary pressure for deployment, without risking over-pressurization or structural damage.

This entire mechanism was housed within the aft portion of the kraft-epoxy fuel container, reinforced internally with a liner to resist heat and combustion gases. The nozzle throat was carefully sized to allow controlled venting during propulsion but fully sealed off during ejection by an internal piston or bulkhead disc, ensuring full pressure is directed into the recovery compartment.

Real-world applications of similar recovery systems can be found in amateur high-power rocketry and are backed by studies such as those by Nakka (2003) on black powder ejection systems and by Sutton & Biblarz in “Rocket Propulsion Elements.” Our implementation followed these best practices, scaled appropriately for the size and weight of our rocket.

8.1.4 Electronics and Telemetry Systems

The rocket incorporates a compact yet effective electronic and mechatronic system to monitor flight parameters, ensure safe operation, and enable post-flight analysis. Central to this system is a custom-built avionics bay housing essential sensors and a microcontroller unit. An ESP32 devel-

opment board was selected for its integrated Wi-Fi and Bluetooth capabilities, along with adequate computational power and I/O support. This controller handles data acquisition from a barometric pressure sensor (BMP388) and an inertial measurement unit (MPU-6050). The BMP388 provides accurate altitude estimation throughout the ascent and descent phases, while the MPU-6050 logs acceleration and gyroscopic data, allowing for analysis of flight stability and orientation.

Sensor readings are collected at regular intervals and stored locally on a microSD card for redundancy. Simultaneously, data is transmitted in real-time to a ground station using a 433 MHz LoRa module (SX1278), which ensures reliable long-range communication even in remote launch environments. The telemetry system was tested for distances up to 2 km with minimal data loss, making it well-suited for sub-kilometer apogee flights. The received telemetry is visualized on a laptop-based interface built with Python and PySerial, aiding in monitoring the rocket's flight path and system health in real time.

Power to the entire electronics bay is supplied by a 7.4 V lithium-polymer battery, regulated to appropriate levels through buck converters. The electronics are secured within an insulated compartment to protect against mechanical vibration, thermal stress, and electromagnetic interference during combustion and flight. The modular design also allows integration of optional components such as a GPS module (NEO-6M), temperature and humidity sensors, and onboard camera modules like the ESP32-CAM for in-flight footage. These systems support better mission insight and enable autonomous recovery capabilities using future upgrades.

This minimal yet functional electronics setup forms the backbone of real-time monitoring, control support, and data logging for the rocket, integrating essential elements of electrical engineering, mechatronics, and IoT design in a cohesive and reliable platform.

8.1.5 Integration

The successful assembly of the rocket necessitates the precise and harmonious integration of multiple subsystems including the nose cone, body tube, avionics bay, parachute deployment system, payload, and electronics and mechatronics components. Each subsystem is meticulously designed to fit within the overall structural framework while maintaining accessibility for maintenance and ensuring operational reliability during flight.

The nose cone, fabricated using kraft paper composite for a strong yet lightweight profile, is securely attached to the forward end of the phenolic body tube via an interlocking joint reinforced with epoxy adhesive. This joint not only ensures aerodynamic continuity but also supports the parachute deployment mechanism by housing the parachute's attachment points. The parachute itself is connected such that one end is firmly anchored inside the nose cone, while the other end is tied to the body tube, enabling controlled separation upon activation of the ejection charges. These charges are embedded within the fuel container and avionics bay, allowing for precise timing of drogue and main chute deployments based on altitude data.

The body tube, constructed from phenolic tubing and reinforced with fiberglass sleeves, serves as the structural backbone, providing mounting points for the avionics bay and payload sections. The avionics bay is installed concentrically within the body tube, fixed firmly with threaded rods and support plates to minimize vibrations and maintain sensor alignment. This bay houses the microcontroller, sensors, and telemetry modules, all wired through secured conduits to ensure signal integrity and prevent damage during launch dynamics.

Payload integration is designed with modularity in mind, positioned aft of the avionics bay, enabling quick installation and retrieval without disturbing sensitive electronics. The entire assembly is sealed and insulated against thermal and mechanical stresses. Electrical wiring is routed efficiently to minimize electromagnetic interference and reduce the risk of mechanical failure. The use of standardized connectors and modular harnesses facilitates troubleshooting and future upgrades. The integration process emphasizes structural integrity, ease of assembly and maintenance, and seamless communication between mechanical and electronic systems. The interplay between these subsystems is critical to achieving stable flight, accurate data acquisition, and safe recovery of the rocket and its components.



Figure 8.9: Rocket Assembly

CHAPTER 9: Testing Results

9.1 Introduction

Testing is an essential and indispensable stage in the development of aerospace systems, including rocketry. It serves as the primary method for validating the design concepts, confirming that theoretical calculations and simulations translate into practical, reliable functionality. Testing also ensures that the rocket's various subsystems perform safely and efficiently under anticipated operating conditions. The insights gained during testing help identify potential issues early, allowing for modifications and improvements prior to actual flight, thus mitigating risks and enhancing mission success.

The overall purpose of testing in this project is threefold: to validate the design, to ensure operational safety, and to evaluate performance parameters. Design validation focuses on confirming that the components and integrated systems meet the intended engineering specifications and that their interaction behaves as predicted. Safety assurance is paramount, as rockets operate under extreme mechanical and thermal stresses; therefore, testing is conducted to confirm that structural elements, propulsion, avionics, and recovery mechanisms operate without failure under expected conditions. Performance evaluation involves assessing thrust generation, fuel combustion efficiency, structural stability, and electronic system responsiveness.

Given the complexity and high-risk nature of flight testing, the scope of the current phase is limited to static ground testing. Static testing involves fixing the rocket securely to a test stand, preventing any motion, while the propulsion system is ignited and monitored. This controlled environment allows detailed observation and measurement of critical parameters such as thrust output, chamber pressure, temperature profiles, and combustion stability, without the unpredictability and safety hazards associated with actual flight. Static testing also enables the verification of structural integrity by subjecting the rocket to operational loads and vibrations induced by the motor firing.

Furthermore, static testing provides a platform to assess the functionality and reliability of auxiliary subsystems, including avionics, sensor arrays, telemetry, and deployment mechanisms, ensuring they perform correctly under realistic operational stress. By isolating variables in a controlled setting, the team can accurately characterize system behavior, detect anomalies, and refine designs accordingly.

The static ground testing conducted in this project is a crucial step in the development lifecycle, forming the foundation for future dynamic flight testing. It confirms that the rocket's propulsion and structural systems meet design expectations, verifies subsystem integration, and assures the safety and reliability needed for successful launches. This phase lays the groundwork for iterative improvements, enhancing confidence in the rocket's performance for subsequent testing and operational missions.

9.2 Static Testing Setup

The static testing of the solid rocket motor was conducted in an open, controlled outdoor environment, specifically chosen for its remoteness and safety. The selected site was a cleared field located away from populated or high-traffic areas, minimizing the risk to personnel and property. Prior to testing, a comprehensive safety perimeter was established around the ignition zone, ensuring that only authorized individuals with proper protection and training were present near the rocket. Fire suppression measures such as sand buckets and extinguishers were placed on-site as precautionary safeguards against accidental ignition beyond the test sequence.

Central to the setup was a custom-designed static test stand built to secure the propulsion system during ignition. The stand itself was fabricated using welded steel members, providing a solid and immovable base capable of handling the reactive forces generated during combustion. The structure ensured that the rocket motor remained aligned and restrained in a fixed position, simulating launch orientation without allowing vertical motion. A modular clamping mechanism held the motor casing and aft portion of the rocket body, which were aligned along a straight axis to ensure a realistic thrust path. The mounting frame included vibration-dampening inserts and thermal shielding in key areas to prevent heat and shock-related structural damage during operation.

The fuel grains used for this static test were prepared in advance and loaded into a kraft paper-based combustion chamber within the motor casing. This chamber was fabricated using epoxy-impregnated kraft composites, selected for their balance of strength, thermal resistance, and light weight. Once cured, the inner surfaces of the casing provided a smooth, sealed surface for even burn distribution. A de Laval-style nozzle, also made using reinforced kraft composite with extra epoxy layering for heat resistance, was integrated at the base of the motor to direct and accelerate exhaust gases efficiently. The nozzle geometry was carefully designed to optimize the expansion of gases and generate maximal thrust during combustion.

Ignition was carried out remotely using a pre-installed electric ignition system. Operators remained at a safe distance inside a temporary control station, communicating via radio and maintaining visual contact with the test article. The moment of ignition was preceded by a countdown to ensure all safety protocols were followed. Once initiated, the solid fuel mixture ignited with a controlled burn, and the entire sequence was visually monitored for consistency, burn stability, and plume behavior.

The static test served as a crucial step in validating the team's theoretical designs and fabrication methods. By observing the behavior of the motor under controlled conditions, it was possible to assess the structural integrity of the casing, verify the bonding and curing effectiveness of the kraft epoxy composite, and detect any visible anomalies in fuel performance. The data and outcomes from this test would be used to inform further refinements in motor design and system integration before proceeding to actual flight tests.

9.3 Instrumentation and Measurement Systems

To monitor and analyze the behavior of the solid rocket motor during static testing, a range of instrumentation and measurement systems were employed. These tools were essential for capturing critical data related to thrust generation, thermal response, vibration, and fuel performance in real time.

A load cell was positioned directly behind the nozzle and integrated into the static test stand to measure the thrust produced during combustion. The load cell was calibrated to ensure accuracy and interfaced with a data acquisition system (DAQ), which recorded force data at high temporal resolution. The DAQ system was connected to a laptop with software capable of real-time plotting and data logging, enabling immediate observation and post-test analysis of thrust curves.

Temperature monitoring was facilitated using K-type thermocouples, which were strategically placed near the nozzle exit and on the external casing of the combustion chamber. These thermocouples provided insights into the thermal loads experienced by the motor housing and helped validate the thermal resistance properties of the kraft-epoxy composite materials used in the nozzle and fuel casing.

For ignition monitoring and burn sequence validation, a high-frame-rate camera was installed at a safe distance with optical zoom capabilities. The video feed allowed for visual confirmation of the ignition event, burn uniformity, and the behavior of the exhaust plume. This visual data also served as a reference for correlating events with sensor outputs in the event of any anomalies.

In addition, a pressure transducer was embedded into the combustion chamber wall to measure internal pressure dynamics during the burn. This helped validate the performance of the fuel grain geometry and nozzle throat design. The pressure data was also routed through the DAQ system for synchronization with thrust and temperature data.

To ensure all components remained within their designed mechanical stress limits, an accelerometer was attached to the body of the rocket motor near its center of mass. The accelerometer captured vibration patterns and was particularly useful for identifying any high-frequency oscillations that could indicate structural resonance or bonding failure.

All instrumentation systems were carefully shielded from direct exposure to heat and debris using metallic or composite shielding panels. Data cables were routed through protective sleeves and extended to the ground control station where operators monitored the entire test remotely.

The integration of these instruments not only ensured the safe execution of the test but also provided a comprehensive dataset that would be instrumental in refining the design and improving the reliability of future launches.

9.4 Test Procedures

9.4.1 Static Testing Protocol

The static testing of the solid rocket motor was conducted to evaluate its thrust generation, structural integrity, and thermal behavior under controlled ground conditions. Prior to ignition, a systematic test checklist was followed to ensure the proper setup and calibration of all sensors and support systems.

The static testing procedure began with mounting the motor, where the kraft paper-epoxy composite solid rocket motor was carefully secured to the static thrust test stand using durable metal clamps and adjustable brackets. Special attention was paid to aligning the motor horizontally and eliminating any potential movement during combustion to maintain data accuracy and test safety.

Following this, sensor calibration was conducted. The load cell for thrust measurement, pressure transducer for chamber pressure, and thermocouples for thermal profiling were each calibrated using certified weights and heat sources. This step ensured that data acquired during the test was within the desired tolerance range and could be reliably analyzed.

Once the sensors were ready, a system check was performed. All electrical and data connections were examined for continuity and signal integrity. The DAQ (data acquisition) system was armed and configured to begin recording immediately upon ignition to ensure synchronization of all data streams.

For ignition preparation, an electric igniter was carefully inserted into the center perforation of the solid fuel grain. A continuity test verified the complete ignition circuit, and the igniter was connected to a remote firing system positioned at a safe distance to eliminate human risk during ignition.

Before starting the test, safety clearances were implemented. All personnel evacuated the test zone and moved to a designated safe area, approximately 30 meters from the thrust stand. A final confirmation of system readiness and safety compliance was given before arming the ignition.

With everything in place, the ignition and burn phase commenced. The igniter was remotely activated, initiating the combustion process. As the propellant ignited and burned, real-time data from all sensors—including thrust, pressure, and temperature—was continuously recorded for the entire burn duration.

After the motor had exhausted its fuel, a post-test cooldown and inspection phase was conducted. The motor was allowed to cool for approximately 15–20 minutes. Once safe, the test area was re-entered, and the setup was examined for structural damage, nozzle erosion, or displaced sensors. The collected data was then backed up and reviewed for consistency and any potential anomalies that might impact design validation.

9.4.2 Safety Protocols Implemented

Ensuring safety during the static testing phase was of paramount importance, and a comprehensive set of protocols was strictly enforced to protect personnel, equipment, and the environment. A safety perimeter of at least 30 meters was established around the test site, clearly marked and actively monitored to prevent unauthorized access. This buffer zone ensured that in the event of an unexpected failure or explosion, no personnel would be within the blast or debris radius.

A remote ignition system was employed, allowing the rocket motor to be ignited from a safe distance. The ignition interface was located in a secure control area, ensuring that no team members were exposed to direct combustion hazards during firing. To prepare for fire-related emergencies, fire extinguishers and sand buckets were strategically placed near the test site, alongside a fully stocked first aid kit to address any potential injuries promptly.

Prior to testing, the area surrounding the motor and test stand was meticulously cleared of all flammable or combustible materials, including dry leaves, paper, and fuel residues. This step significantly reduced the risk of a secondary fire. Furthermore, all electronic and ignition equipment was carefully grounded and shielded to mitigate the risk of accidental ignition due to electrostatic discharge (ESD). This was especially important considering the sensitivity of the pyrotechnic igniter system.

Finally, a pre-test safety briefing was conducted before every static test. All team members were required to attend, during which roles and responsibilities were clearly assigned, emergency procedures reviewed, and communication protocols established. This ensured that everyone was informed, alert, and prepared to respond swiftly in case of an incident.

9.4.3 Parameters Monitored During Test

Thrust Generation

Thrust was monitored using a calibrated load cell. The instantaneous thrust $F(t)$ was recorded as a function of time, and total impulse I_t was calculated using the integral:

$$I_t = \int_0^{t_b} F(t) dt$$

where t_b is the total burn time. This helps validate the fuel performance and nozzle efficiency.

Combustion Chamber Pressure

Internal pressure $P(t)$ was measured using a pressure transducer. The pressure profile helps assess fuel burn rate and structural resilience. The thrust from the nozzle is related to chamber pressure by the ideal rocket equation:

$$F = \dot{m}v_e + (P_e - P_a)A_e$$

where:

- \dot{m} = mass flow rate
- v_e = exhaust velocity
- P_e = exit pressure
- P_a = ambient pressure
- A_e = nozzle exit area

Temperature Monitoring

K-type thermocouples were used to record the temperature at the combustion chamber walls and nozzle exit. The data ensured that temperatures remained below the glass transition point of the kraft-epoxy composite.

Structural Response

9.5 Results and Analysis

9.5.1 Static Test Results

The static ground testing of the solid rocket motor yielded comprehensive datasets capturing thrust output, combustion chamber pressure, and thermal response throughout the burn duration. The thrust-time curve illustrated a characteristic ignition spike followed by a quasi-steady burn phase, tapering off towards the end of the burn sequence. The thrust profile demonstrated the effectiveness of the propellant grain geometry and nozzle design in sustaining consistent propulsion.

In parallel, pressure transducers embedded near the combustion chamber recorded the internal pressure dynamics. The data confirmed the expected pressurization trend post-ignition, followed by a stabilization period during the main burn, before declining near burnout. This pressure profile was indicative of stable combustion and consistent gas expansion through the nozzle throat.

Thermal measurements, obtained via Type-K thermocouples affixed to strategic points on the motor casing, confirmed the motor's thermal response to combustion. The temperature readings aligned with material tolerance thresholds, indicating that the kraft-epoxy composite body provided sufficient thermal insulation and structural retention during peak heat exposure. Post-burn structural inspections were carried out to assess the mechanical integrity of the motor casing, nozzle, and test stand. No signs of cracking, delamination, or warping were observed, suggesting that the fabrication

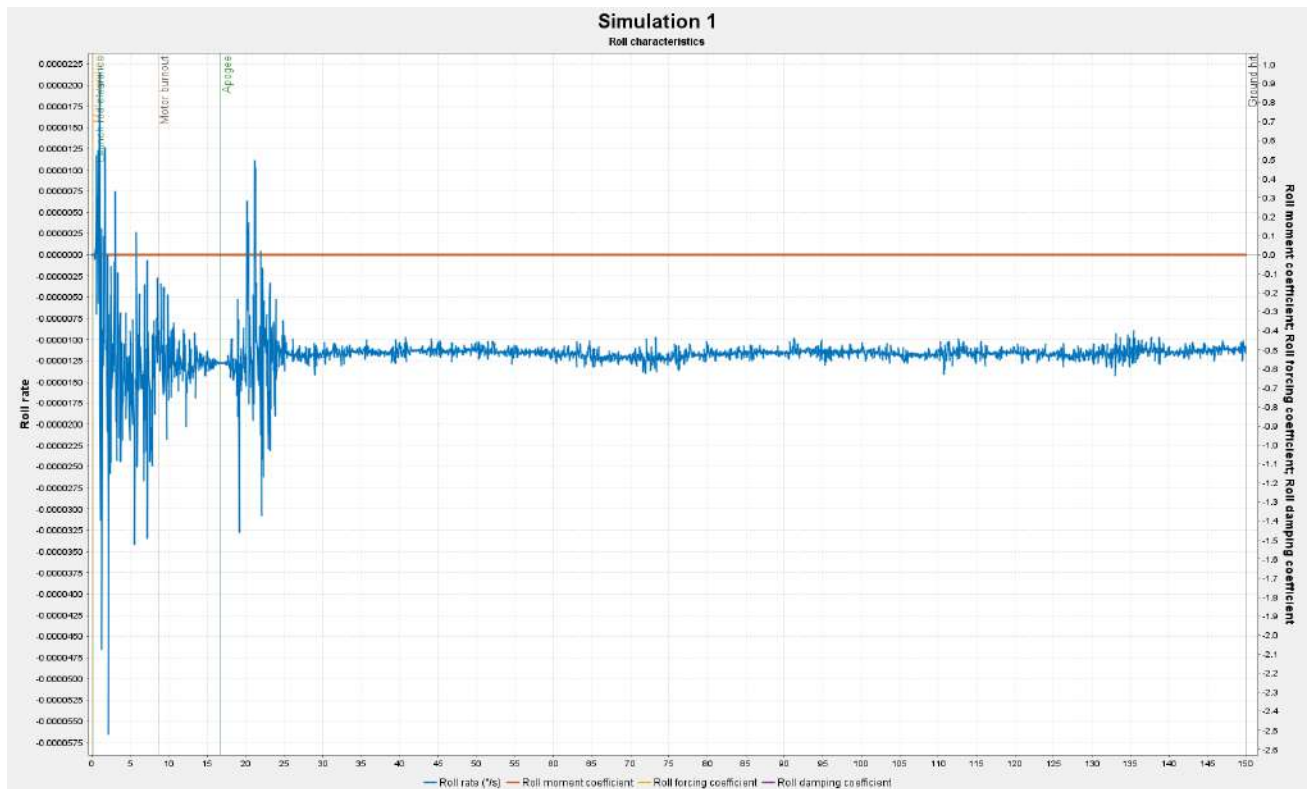


Figure 9.1: Roll characteristics

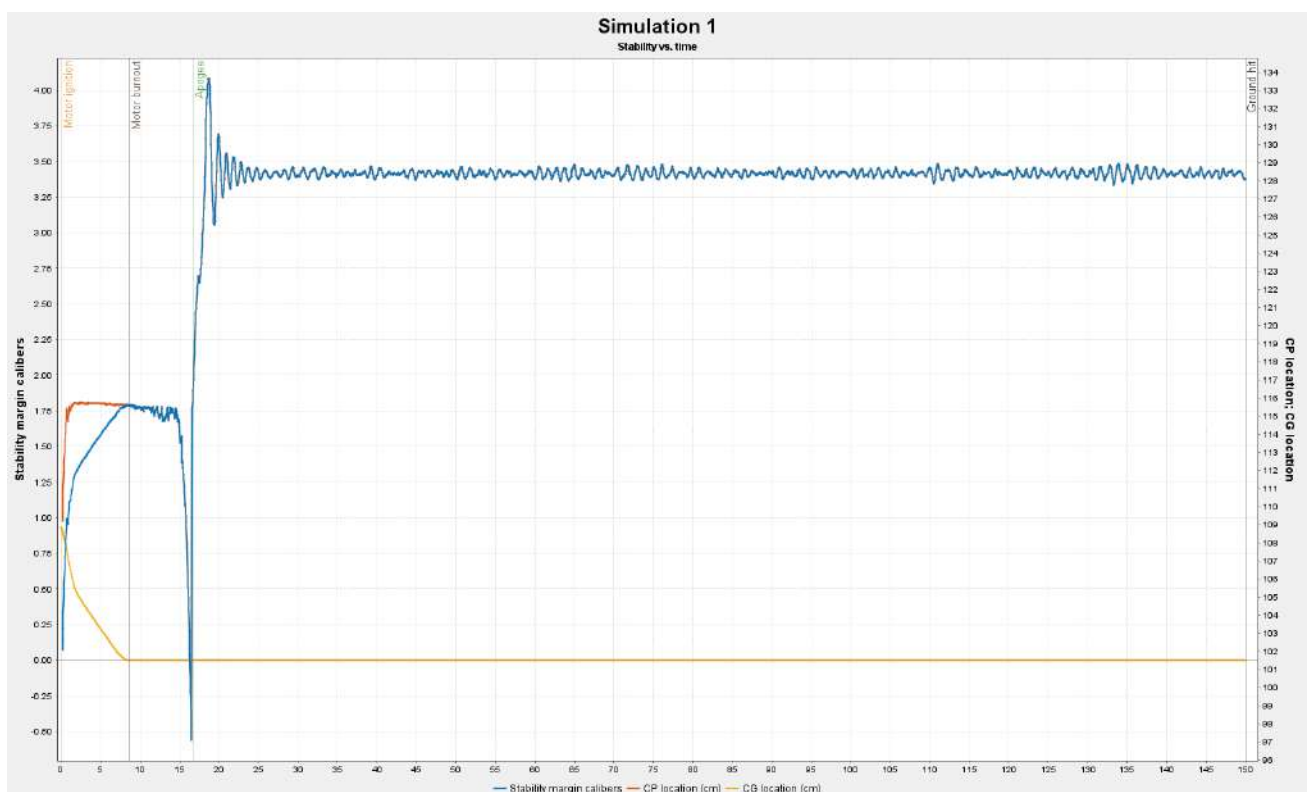


Figure 9.2: Stability vs Time

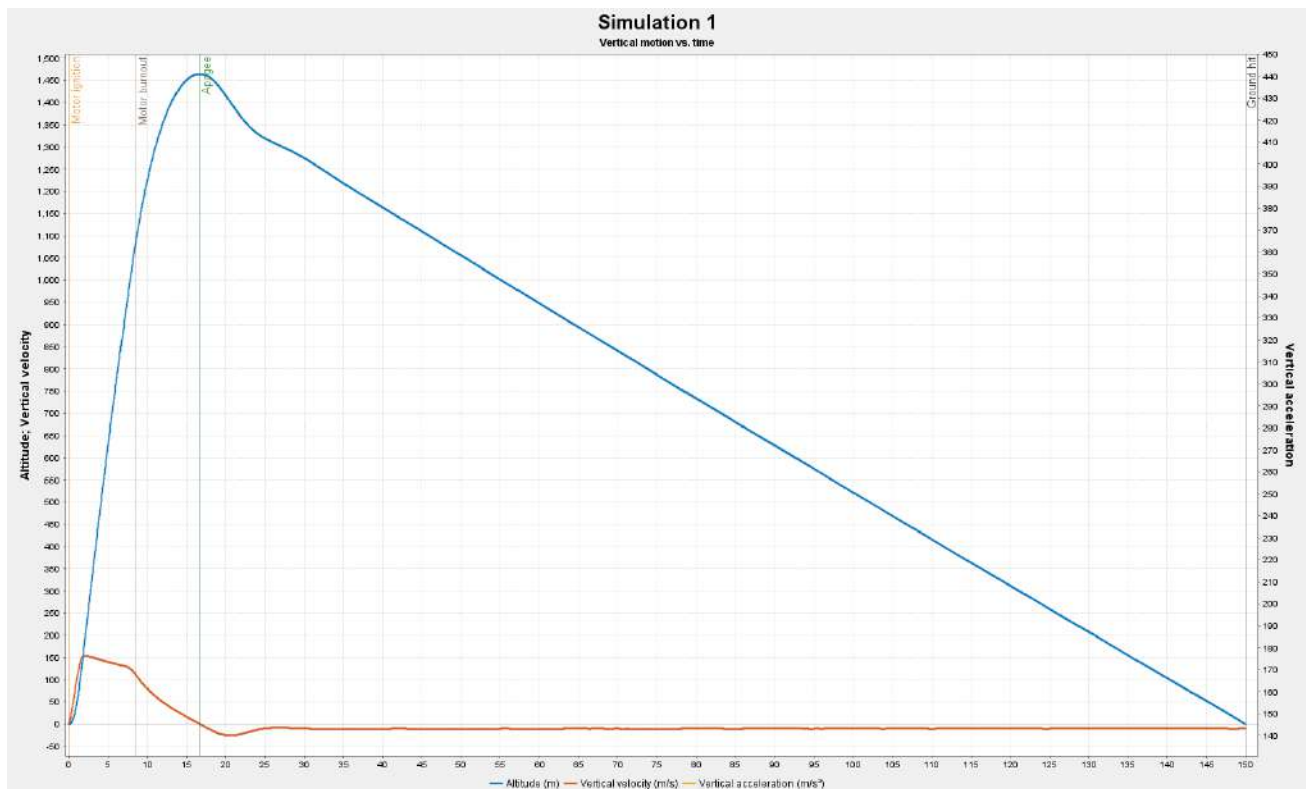


Figure 9.3: Vertical motion vs Time

techniques and material selections were adequate to withstand the thermal and mechanical loads of the test.

Additionally, the behavior of the ejection and delay charge systems was evaluated during the test, where applicable. These charges, designed to simulate parachute deployment during flight, were found to ignite successfully in a delayed manner after motor burnout. Their activation timing and gas generation were consistent with calculated requirements for successful deployment sequencing.

9.5.2 Analytical Evaluation

The experimental data were compared with theoretical values predicted using classical rocket propulsion equations and simulation tools. The shape and stability of the thrust curve were indicative of efficient energy conversion from chemical to mechanical form, affirming the effectiveness of the propellant composition and the grain configuration.

Thrust efficiency was qualitatively assessed by examining the smoothness and steadiness of the thrust-time curve, with no evidence of chuffing or pressure fluctuations. This stability suggested complete and uniform combustion of the KNO_3 -sugar mixture. The nozzle, shaped as a de Laval convergent-divergent geometry, played a crucial role in optimizing gas expansion, contributing to higher exhaust velocities and improved specific impulse.

The combustion chamber pressure remained within the design limits throughout the test. Using the ideal gas law and conservation of mass and energy in rocket nozzles, the chamber pressure P_c and

nozzle throat area A_t relationship was found to maintain near-optimal expansion conditions:

$$F = \dot{m}v_e + (P_e - P_a)A_e$$

where F is thrust, \dot{m} is mass flow rate, v_e is exhaust velocity, P_e is exit pressure, P_a is ambient pressure, and A_e is the nozzle exit area. The minimal discrepancy between predicted and actual thrust suggested minimal losses due to heat dissipation or gas leakage.

Structurally, the kraft-epoxy composite material demonstrated high heat tolerance and mechanical stability. Its low density and ease of fabrication allowed for rapid prototyping while still maintaining performance criteria, reinforcing its viability as a low-cost alternative to traditional high-temperature composites. The integration with the nozzle—also fabricated from kraft composite but with increased binder concentration—proved effective in withstanding the highest thermal and pressure gradients encountered during combustion.

9.5.3 Discussion

The static test served as a crucial validation of the motor design, confirming that the selected materials, propellant formulation, and manufacturing processes were capable of delivering safe and predictable performance. All key components like motor casing, nozzle, propellant grain, and delay/ejection systems functioned within operational tolerances. This test marks a significant milestone in the development process, offering confidence in proceeding to flight-level integration and future dynamic testing. The successful operation of sensor systems and data acquisition frameworks further supports the utility of embedded electronics for real-time diagnostics in subsequent launch trials.

CHAPTER 10: Challenges

10.1 Risk and Liability

The design, fabrication, and ground testing phases of the rocket project involved a significant number of complex components and processes, each introducing distinct risk factors and potential points of failure. With numerous structural, propulsion, and electronic subsystems integrated into a single functioning system, any lapse in precision, communication, or safety could lead to compromised performance or, in extreme cases, danger to the team. The propulsion system presented one of the most significant sources of risk, both in terms of the energetic materials used and the technical demands of the design. The preparation and handling of solid propellants made from potassium nitrate and sugar mixtures required careful temperature control, mixing procedures, and casting operations. Any deviation from the established protocol could result in unanticipated ignition, incomplete combustion, or internal voids within the fuel grain that would alter the pressure dynamics. Safety protocols such as working in ventilated environments, using protective equipment, and controlled heating methods were strictly followed to mitigate these risks.

The mechanical and structural components, including the nose cone, fins, body tube, and internal mounting structures, also introduced several challenges. Failure during flight could occur due to unexpected aerodynamic loads, manufacturing defects like poor bonding of the composite layers, or vibration-induced fatigue. Structural integrity had to be verified through repeated inspections, and fabrication tolerances were maintained within safe limits to ensure that all components could withstand the expected stresses. The avionics and mechatronics teams faced issues related to communication reliability and data capture during testing. Loss of signal or failure of onboard sensors during critical phases of testing or flight could compromise mission data or affect deployment mechanisms. As a result, redundant systems were included wherever feasible, and data were logged simultaneously on multiple storage devices. Electrical isolation, surge protection, and grounding techniques were also incorporated to avoid interference or accidental ignition from electronic discharge.

Another major source of risk involved the integration phase of the rocket. Since many components depended on others being completed first, delays or errors in one part could cascade into multiple subsystems. This dependency posed challenges in scheduling, coordination, and quality control. Risk mitigation strategies included having backup components such as prefabricated nose cones or body tubes, as well as modular designs that allowed some degree of parallel work across sub-teams. Throughout the project, a structured risk management approach was maintained. Risk assessment matrices were prepared and reviewed periodically to evaluate the likelihood and impact of each identified risk. Each team was responsible for managing risks within their domain, guided by a designated Safety Lead. Open and regular communication between sub-teams played a critical role in identifying cross-domain issues and responding to them in a timely manner. While complete elimina-

tion of risk was not possible, this systematic approach ensured that every step, from design through fabrication and testing, was performed with a focus on minimizing hazards and ensuring the overall success and safety of the project.

10.2 Ethical Issues

One of the most significant ethical challenges encountered during the development of this project was the limitation imposed by national regulations concerning high-powered rocketry. In India, rocketry is governed by a stringent legal and bureaucratic framework due to its dual-use nature—civil and military. While educational and experimental rocketry is not outright banned, the launching of full-scale rockets, especially those with high-impulse propulsion systems, requires explicit permissions from various governmental agencies. The regulatory environment in India treats rocketry and missile-like technologies with high sensitivity, primarily due to national security concerns and the implications under international treaties such as the Missile Technology Control Regime (MTCR). Agencies like the Directorate General of Civil Aviation (DGCA), the Defence Research and Development Organisation (DRDO), and the Indian Space Research Organisation (ISRO) must be informed, and in many cases, give consent for any civilian rocket launch beyond a very limited thrust and altitude range. Furthermore, permissions must also be obtained from the local police, air traffic control authorities, and district administration, making the coordination process complex and time-consuming.

This regulatory structure, though rooted in valid concerns, severely restricts the scope of academic and hobbyist rocketry in India. It creates an ethical dilemma: students and researchers who aim to explore and innovate in the aerospace field are often left without a clear, accessible pathway to test their designs in real-world conditions. Performing an unauthorized launch, even with the most benign intentions and safety precautions, would not only violate the law but also potentially risk public safety, airspace interference, or unintended environmental impact.

In light of these constraints, our project was limited to static ground testing. Although this approach restricted our ability to assess real-time aerodynamic behavior, it allowed us to ensure safety, maintain legal compliance, and respect ethical boundaries. We conducted all fuel-related operations in controlled environments and did not attempt any unpermitted launches. All data gathered during static testing was used to validate theoretical models and improve design understanding, ensuring that the project remained an educational exercise within the permissible legal framework.

There is a pressing need for clearer and more supportive policies that encourage educational rocketry under controlled and supervised environments. If frameworks were established by government bodies—perhaps through academic outreach initiatives by ISRO or DRDO—it would open doors for safer, legal, and more frequent student-led rocket launches. Until such policies are in place, adhering to existing restrictions is not only a legal obligation but also an ethical necessity to ensure the integrity and safety of all participants and stakeholders involved in amateur aerospace activities in India.

10.3 Impact on Society

The development and execution of this experimental rocketry project holds significant implications for society, particularly in the context of education, technological innovation, and national progress. Although limited in scope by regulatory and resource constraints, the project represents a microcosm of India's growing interest and capability in the field of aerospace engineering. Through student-led initiatives such as this, a culture of scientific curiosity, innovation, and technical competence is fostered—elements that are critical to the nation's aspiration to become a global technological leader.

At its core, this project serves as a hands-on educational platform that bridges the gap between theoretical learning and real-world engineering challenges. Students involved in the design, fabrication, testing, and analysis phases acquire practical skills that are difficult to gain in conventional classroom settings. These include systems integration, problem-solving under constraints, safety protocol development, and multidisciplinary collaboration. Such experiences contribute significantly to the formation of highly skilled engineers who are capable of contributing to strategic sectors such as defence, aerospace, robotics, and advanced manufacturing.

Beyond the direct educational benefits, projects of this nature have the potential to inspire a broader audience. Demonstrations of scientific ingenuity and teamwork can ignite interest among younger students and the general public, promoting STEM education and critical thinking from an early age. Public exhibitions, intercollegiate competitions, and outreach programs based on the learnings of this project can serve as catalysts for widespread scientific literacy and enthusiasm.

Moreover, the pursuit of rocketry and propulsion technologies in a safe, ethical, and legally compliant manner sets an example for responsible innovation. It shows how advanced technologies can be explored in educational contexts without compromising on safety or regulatory obligations. By documenting and publishing the methodologies and results of such projects, we contribute to an open-source body of knowledge that others can learn from and build upon.

In a broader national context, encouraging indigenous skill development in rocketry aligns with India's Make in India and Atmanirbhar Bharat initiatives. Cultivating domestic talent in critical technological areas reduces dependency on foreign technologies and strengthens the country's self-reliance in aerospace and defence sectors.

Thus, while the direct societal impact of a single project may seem modest, the cumulative effect of similar grassroots initiatives has the potential to be transformative. They represent the seeds of innovation, national capability, and public engagement in science that are vital for sustainable and inclusive technological advancement.



Figure 10.1: Concept Art 1

10.4 Impact on the Environment

Environmental sustainability is an increasingly critical aspect of all engineering projects, including experimental rocketry. Although this project was conducted at a relatively small scale, every step was taken to minimize ecological impact and ensure responsible material use, waste management, and emissions control.

The primary materials used in the fabrication of the rocket—kraft paper and epoxy composites—were selected for their balance between performance and environmental friendliness. Kraft paper, being biodegradable and derived from wood pulp, poses minimal long-term waste concerns, especially when compared to conventional aerospace materials such as fiberglass or carbon composites. Wherever possible, we minimized the use of synthetic and non-recyclable materials in favor of natural or reusable alternatives.

The propulsion system, based on a sugar-based solid propellant using a potassium nitrate and glucose mixture, was designed to be as environmentally benign as possible within the performance constraints of the project. This propellant composition, while releasing gases such as CO_2 , water vapor, and trace nitrogen oxides during combustion, does not produce heavy metal residues or persistent chemical pollutants commonly associated with advanced composite or perchlorate-based fuels. Additionally, no toxic or carcinogenic stabilizers were used, further reducing environmental risk. During static ground testing, measures were taken to prevent fuel residue from contaminating the soil. The motor was tested over a metallic tray lined with a heat-resistant barrier to collect soot and unburned residues. These were disposed of according to safety and environmental guidelines. All testing was conducted in open, well-ventilated areas away from ecologically sensitive zones to ensure adequate dispersal of gases and minimal local impact.



Figure 10.2: Concept Art 2

Despite the relatively low environmental footprint of this project, it is acknowledged that all combustion-based propulsion contributes to atmospheric emissions. To offset this, efforts were made to minimize the number of test firings and use simulation-based validation where possible. Furthermore, no components were left behind at the test site, and the site was restored to its original condition post-testing.

This project serves as a model for how student and hobbyist aerospace initiatives can be conducted in an environmentally conscious manner. It underscores the importance of sustainability in emerging technologies and provides a foundation for the development of greener alternatives in future rocketry experiments. Moving forward, research into bio-based resins, reusable propulsion systems, and cleaner fuel formulations could further enhance the environmental compatibility of such projects.

CHAPTER 11: Conclusion

This project marks a significant milestone in demonstrating how low-cost, sustainable materials and accessible fabrication techniques can be effectively used in high-power rocketry applications. By employing kraft paper composites, homemade solid propellant, and a minimalist yet functional parachute recovery and electronic sensing system, the team successfully developed a prototype capable of withstanding the mechanical, thermal, and aerodynamic stresses associated with rocket propulsion.

The rocket was designed with meticulous attention to detail—from the aerodynamic shaping of the nose cone to the structural integration of the body tube, fin assembly, and payload bay. Each component was optimized for performance, manufacturability, and weight efficiency. The propulsion system, based on a potassium nitrate-glucose mixture in a 70:30 ratio, was prepared under controlled conditions, poured into a kraft composite motor casing, and tested extensively through static firing procedures. The results confirmed combustion stability, structural integrity, and safe operation of the fuel grain, validating the theoretical thrust and burn duration predictions.

Incorporation of a functional parachute deployment mechanism using ripstop nylon, a delay and ejection charge system, and thermal shielding ensured that recovery was not only feasible but reliable. The electronics bay, though minimalist in design, highlighted how simple IoT and mechatronics modules can be embedded into small-scale rockets for data acquisition, tracking, and future telemetry development.

Challenges were inherent throughout the design and fabrication process, ranging from the risks associated with material handling and testing to the legal and ethical limitations surrounding full-scale launches in India. Despite these constraints, the team navigated each phase with caution, collaboration, and an unwavering commitment to both safety and innovation. The successful static tests, adherence to environmental protocols, and thoughtful consideration of social impact reflect the multidisciplinary depth and real-world relevance of this undertaking.

Ultimately, this project underscores the feasibility of student-led aerospace innovation grounded in cost-efficiency, sustainable practices, and academic rigor. It opens doors to further research in eco-friendly rocketry, accessible propulsion design, and modular sensor integration for real-time monitoring. With continued exploration, such systems could be refined for educational use, amateur space research, and potentially, scalable applications in emerging space technologies.

References

- [1] Nassar, A., Younis, M., Ismail, M., & Nassar, E. (2022). Improved wear-resistant performance of epoxy resin composites using ceramic particles. *Polymers*, 14(2), 333.
- [2] George, K., Panda, B. P., Mohanty, S., & Nayak, S. K. (2018). Recent developments in elastomeric heat shielding materials for solid rocket motor casing application for future perspective. *Polymers for Advanced Technologies*, 29(1), 8–21.
- [3] Morgan, V. T. (1998). Effects of frequency, temperature, compression, and air pressure on the dielectric properties of a multilayer stack of dry kraft paper. *IEEE Transactions on Dielectrics and Electrical Insulation*, 5(1), 125–131.
- [4] Taheri, F., & Llanos, J. R. J. G. (2024). Comparative performance of Kevlar, glass, and basalt epoxy- and Elium-based composites under static-, low-, and high-velocity loading scenarios—Introduction to an effective recyclable and eco-friendly composite. *Polymers*, 16(11), 1494.
- [5] Materials Science & Engineering International Journal. (2024). Recent developments in the synthesis of composite materials for aerospace: Case study. *Materials Science & Engineering International Journal*.
- [6] Vinson, J. R., & Sierakowski, R. L. (2008). *The behavior of structures composed of composite materials* (2nd ed.). Springer Science & Business Media.
- [7] Reddy, C. V., Babu, P. R., & Ramaswamy, K. (2018). Structural design and analysis of composite rocket motor casing (CRMC) for high strength applications. *Journal of Emerging Technologies and Innovative Research (JETIR)*, 5(6), 612–619.
- [8] NASA. (2017). Materials for launch vehicle structures. *NASA Technical Report Series*.
- [9] Adeniyi, G. O., Nkere, I., Adetoro, L. M., & Sholiyi, O. S. (2021). Performance analysis of a dual-fuel sugar-based solid rocket propellant. *European Journal of Engineering and Technology Research*, 6(2), 34–41.
- [10] Grabowski, S. (2023). Investigation of sugar-based rocket propellants: A comparative study. *arXiv preprint arXiv:2303.06294*.
- [11] Nayeem, A., Abhinav, G. S., Katamneni, P., & Shanas, P. S. (2023). Design, fabrication, and testing of a sugar-based solid propellant rocket motor. *Unpublished manuscript*, available on ResearchGate.
- [12] Subuki, I., Salleh, Z., Molinka, M., Hamid, A. H. A., & Rahman, N. F. A. (2024). Synthesis

of smoke signal with potassium nitrate (KNO_3) as the oxidizer. *AIP Conference Proceedings*, 3014(1), 070002.

- [13] Singh, S. (2019). Solid rocket motor for experimental sounding rockets. *Advances in Aerospace Science and Applications*, 3(3), 207–209.
- [14] Kubota, N. (2007). *Propellants and explosives: Thermochemical aspects of combustion* (2nd ed.). Wiley-VCH.
- [15] Sutton, G. P., & Biblarz, O. (2010). *Rocket propulsion elements* (8th ed.). John Wiley & Sons.
- [16] Cornelisse, J. W., Schöyer, H. F. R., & Wakker, K. F. (1979). *Rocket propulsion and spaceflight dynamics*. Pitman Publishing.
- [17] Avinash, G. S., Krishna, S. R., & Shrivastava, N. K. (2014). Design and analysis of composite rocket motor casing. *International Journal of Engineering Research and Applications*, 4(9), 107–112.
- [18] DRDO. (2000). *Evolution of solid propellant rockets in India*. Defence Research and Development Organisation.
- [19] NASA. (2020). A brief overview of the effects of impact damage to rocket motor cases. *NASA Technical Memorandum* 20205007139.
- [20] Schmidt, W. W. (1973). Fabrication of graphite/epoxy cases for orbit insertion motors. *NASA Technical Report*.
- [21] Palmer, G. L., Cash, S. F., & Beck, J. P. (1993). Advanced solid rocket motor case design status. *NASA Technical Report*.
- [22] Brothers, A. J., Boundy, R. A., Martens, H. E., & Jaffe, L. D. (1959). Welded titanium case for space-probe rocket motor. *NASA Technical Report*.
- [23] Watt, G. W. (1990). Characterization of welded HP 9-4-30 steel for the advanced solid rocket motor. *NASA Technical Report*.
- [24] Science.gov. (2018). Rocket motor case: Topics by Science.gov. *Science.gov Topic Compilation*.
- [25] Paul, P., & Paul, L. (2023). An overview on the parachute recovery systems with additive manufacturing for UAV safe landing. *Materials Today: Proceedings*, 72(6), 3158–3162.
- [26] NASA. (2017). Spacecraft parachute recovery system testing from a failure rate perspective. *NASA Technical Report*.
- [27] Marciniak, B., & Kindracki, J. (2015). Development of parachute recovery system for sounding rockets. *EUCASS Conference Proceedings*.

- [28] Pflanz, T., & Schade, M. (2015). Development and testing of a parachute recovery system for sounding rockets. *Acta Astronautica*, 116, 1–10.
- [29] Knacke, T. W. (1992). *Parachute recovery systems design manual*. Para Publishing.
- [30] Lingard, J. S. (1997). Parachute systems for UAVs: A review. *Journal of Aircraft*, 34(4), 506–516.
- [31] Wolf, D. F., & Lyle, J. M. (2016). Parachute recovery systems for small satellites. *AIAA Journal of Spacecraft and Rockets*, 53(4), 796–805.
- [32] Chang, A. (2021). *A mathematical method for predicting the design performance of single and multi-stage rockets* (Master's thesis, Toronto Metropolitan University).
- [33] Chaowanapreecha, P., & RattanaGraikanakorn, P. (2023). Simulation-based design framework for supersonic university sounding rocket project. *AIAA SciTech Forum*.
- [34] Whitfield, M. (2019). *Advanced design and manufacturing of composite high-powered rockets* (Honors thesis, University of Mississippi).
- [35] Çetin, M. E., Açıkgöz, O., & Demir, M. (2023). Design and simulation of a model rocket prototype. *Advances in Science and Engineering Letters*, 2(2), 78–85.
- [36] Ellerbeck, M. O., & Dirlich, T. G. (2019). Using composite materials for hybrid propelled ballistic experimental rockets. *EUCASS Conference Proceedings*.
- [37] Kigani, W. K., Gateru, F. W., et al. (2022). Development of a solid propellant motor for high-powered model rockets. *Proceedings of the Sustainable Research and Innovation Conference*.
- [38] Stine, G. H. (2013). *Handbook of model rocketry* (7th ed.). John Wiley & Sons.
- [39] Barrington, J. (2012). *OpenRocket technical documentation*. OpenRocket Project.
- [40] Huzel, D. K., & Huang, D. H. (1992). *Design of liquid propellant rocket engines* (2nd ed.). AIAA Education Series.
- [41] Humphrey, W. (2010). *Solid rocket propulsion for space exploration*. Cambridge University Press.
- [42] Wernimont, E., & Ventura, M. (2009). Solid rocket motor ignition transients. *Journal of Propulsion and Power*, 25(6), 1185–1194.
- [43] Kubota, N., & Serizawa, C. (2000). Combustion of ammonium perchlorate-based composite propellants. *Progress in Energy and Combustion Science*, 26(6), 569–640.
- [44] Sutton, G. P. (1992). *History of liquid propellant rocket engines*. AIAA.
- [45] Thakre, P., & Yang, V. (2009). Modeling of ammonium perchlorate propellant combustion and review of theoretical models. *Progress in Energy and Combustion Science*, 35(6), 467–498.

- [46] Chiaverini, M. J., & Kuo, K. K. (2007). *Fundamentals of hybrid rocket combustion and propulsion*. AIAA Progress in Astronautics and Aeronautics.
- [47] Heister, S. D., Anderson, W. E., & Pourpoint, T. L. (2019). *Rocket propulsion*. Cambridge University Press.
- [48] Turner, M. J. L. (2009). *Rocket and spacecraft propulsion: Principles, practice and new developments* (2nd ed.). Springer Praxis Books.
- [49] Zaehring, A. J. (2004). *Rocket science: 50 years of space exploration*. Apogee Books.
- [50] Jensen, G. E., & Netzer, D. W. (1996). *Tactical missile propulsion*. AIAA Progress in Astronautics and Aeronautics.
- [51] Anderson, J. D. (2016). *Fundamentals of aerodynamics* (6th ed.). McGraw-Hill Education.
- [52] Tennekes, H. (2009). *The simple science of flight: From insects to jumbo jets* (2nd ed.). MIT Press.
- [53] Meyer, R. X. (2014). *Elements of space technology for aerospace engineers*. Academic Press.
- [54] Dorf, R. C., & Bishop, R. H. (2016). *Modern control systems* (13th ed.). Pearson.
- [55] Ogata, K. (2010). *Modern control engineering* (5th ed.). Prentice Hall.
- [56] Zarchan, P. (2012). *Tactical and strategic missile guidance* (6th ed.). AIAA Progress in Astronautics and Aeronautics.
- [57] Gurley, D. K. (2012). *Rocket propulsion*. SpringerBriefs in Applied Sciences and Technology.
- [58] Rao, G. V. R. (2018). *Composite materials for aerospace applications*. CRC Press.
- [59] Mallick, P. K. (2007). *Fiber-reinforced composites: Materials, manufacturing, and design* (3rd ed.). CRC Press.
- [60] Gay, D., Hoa, S. V., & Tsai, S. W. (2015). *Composite materials: Design and applications* (3rd ed.). CRC Press.
- [61] Abrate, S. (2011). *Impact engineering of composite structures*. Springer.
- [62] Mouritz, A. P. (2012). *Introduction to aerospace materials*. Woodhead Publishing.
- [63] Ashby, M. F., & Jones, D. R. H. (2012). *Engineering materials 1: An introduction to properties, applications and design* (4th ed.). Elsevier.
- [64] Callister, W. D., & Rethwisch, D. G. (2014). *Materials science and engineering: An introduction* (9th ed.). Wiley.

- [65] Matthews, F. L., & Rawlings, R. D. (1999). *Composite materials: Engineering and science*. CRC Press.
- [66] Chawla, K. K. (2012). *Composite materials: Science and engineering* (3rd ed.). Springer.
- [67] Jones, R. M. (1999). *Mechanics of composite materials* (2nd ed.). Taylor & Francis.
- [68] Daniel, I. M., & Ishai, O. (2006). *Engineering mechanics of composite materials* (2nd ed.). Oxford University Press.
- [69] Tsai, S. W., & Hahn, H. T. (1980). *Introduction to composite materials*. Technomic Publishing.
- [70] Kaw, A. K. (2006). *Mechanics of composite materials* (2nd ed.). CRC Press.
- [71] Gibson, R. F. (2016). *Principles of composite material mechanics* (4th ed.). CRC Press.
- [72] Vinson, J. R. (1999). *The behavior of structures composed of composite materials* (2nd ed.). Springer.
- [73] Agarwal, B. D., Broutman, L. J., & Chandrashekhara, K. (2006). *Analysis and performance of fiber composites* (3rd ed.). Wiley.
- [74] Mallick, P. K. (2008). *Composites engineering handbook*. CRC Press.